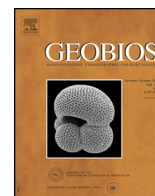




Available online at
ScienceDirect
www.sciencedirect.com

Elsevier Masson France
EM|consulte
www.em-consulte.com



Original article

Late Miocene Erinaceinae from the Teruel Basin (Spain)

Jan A. van Dam^{a,b,*}, Pierre Mein^c, Luis Alcalá^d



^a Faculty of Geosciences, Utrecht University, Vening Meinesz Building A, Princetonlaan 8a, 3584 CB Utrecht, The Netherlands

^b Institut Català de Paleontologia Miquel Crusafont, c/ Columnes s/n Campus de la UAB, 08193, Cerdanyola del Vallès, Barcelona, Spain

^c A.R.P.A., Université Lyon 1, Bâtiment Géode, 69622, Villeurbanne Cedex, France

^d Fundación Conjunto Paleontológico de Teruel-Dinópolis, Av. de Sagunto, 44002 Teruel, Spain

ARTICLE INFO

Article history:

Received 26 November 2019

Accepted 8 June 2020

Available online 7 July 2020

Corresponding editor: Gilles Escarguel

Keywords:

Mammalia
 Erinaceidae
 Dentition
 Function morphology
 Spain

ABSTRACT

Classifying fossil teeth of Erinaceinae (spiny hedgehogs) is a challenging task, because of their scanty record and systematic treatment that heavily relies on skull characteristics. In this paper we describe the complete set of isolated dental elements of Erinaceinae from the upper Miocene sediments of the Teruel Basin (eastern Central Spain). Four different species were recognized: *Postpalerinaceus* cf. *vireti*, *Atelerix* aff. *depereti*, *Atelerix steensmai* nov. sp., and a form classified as Erinaceinae genus and species indet. All four are relatively derived in showing multi-purpose dentitions, not showing only adaptations to insectivory, but also to carnivory, herbivory and possibly durophagy/malacophagy. The temporal occurrence of spiny hedgehogs during the middle to late Miocene in the Teruel Basin and neighboring Calatayud-Montalbán Basin peaks within periods of relative aridity, a correlation consistent with modern geographic distribution. Messinian cooling is the best candidate for explaining a remarkable demise of Erinaceinae at 7 Ma.

© 2020 The Authors. Published by Elsevier Masson SAS. This is an open access article under the CC BY license (<http://creativecommons.org/licenses/by/4.0/>).

1. Introduction

Due to their fragmented fossil record, the phylogenetic history of European spiny hedgehogs (Erinaceinae) remains poorly known (Ziegler, 1999; Engesser, 2009). Although well-preserved cranial material is known from some localities, most of the known mammal sites have yielded either no remains or a few isolated dental elements only. This scarcity is probably due to a combination of their relative rarity within living communities of small mammals and their relative absence in the diet of birds of prey (Reeve, 1994; but see Corbet, 1988), the main agents in accumulating small mammal remains that could finally fossilize (Andrews and Cook, 1990).

The currently accepted view holds that the main evolutionary developments in spiny hedgehogs took place in the Old World (Butler, 1948; Ziegler et al., 2007). The oldest European spiny hedgehog fossils are represented by *Amphechinus arvernensis* Blainville, 1839, a form that occurred in Central/Western Europe during the late Oligocene to earliest Miocene. It soon developed into *A. edwardsi*, Filhol, 1897, as well as into *Dimylechinus bernoullii* Huerzeler, 1944, a side branch restricted to France. The early

Amphechinus species were small-sized, contained relatively rounded skulls with narrow snouts and shallow, elongated mandibles. Their dentition is typically insectivorous, characterized by relatively small teeth that contain many small sharp cusps and ridges, and with rectangularly shaped posterior upper teeth (P4–M2). In many respects, these early European forms resemble their older (early Oligocene to early Miocene) Asian relatives (Ziegler et al., 2007), which were even more primitive in having a well-developed P3, and their third molars not extremely reduced. After a period of apparent absence (including at least the MN3 time interval), new forms entered the European record from the late early Miocene onwards (MN4). Their cranial and dental morphology reflects a broadening of the dietary spectrum: larger size, broader snouts and posterior parts of the skull, deeper mandibles, and upper molars that are more squared.

The generic assignment of these more advanced Miocene forms is still a matter of debate. Confusion stems from the fact that systematic classification in fossil erinaceines depends for a significant part on characters of the skull, which is usually not represented in the fossil material. Apart from *Amphechinus*, species have been generally assigned to three Miocene genera: *Mioechinus*, *Postpalerinaceus*, and *Atelerix*. This number can probably be reduced to two, when more diagnostically relevant material becomes available (see also Engesser, 2009; Ziegler, 2005).

* Corresponding author.

E-mail address: j.a.vandam@uu.nl (J.A. van Dam).

The genus *Mioechinus* was erected by Butler (1948) to distinguish skull material of an intermediate- to large-sized form from Öhningen (*M. oeningensis*, MN7-8) from that of the primitive genus *Amphechinus* as well as that from modern Erinaceinae. Butler based himself mainly on the morphology of the palate (presence of a basisphenoid groove), on the condylar morphology, and on dental features (relative size to M1 of P4, M2 and I1). Another skull feature, the shape of the orbital region (with the lacrimal foramen and the P4 placed anteriorly), was used together with various dental features by Engesser (1980) to separate similarly-aged Anatolian material (the small-sized *M. tobieni* from Yeni-Eskihisar, MN7-8) from *Amphechinus*. It was provisionally assigned to *Mioechinus* based on dental characters. Subsequently, the name *Mioechinus* was also used for similarly-aged material from China (Qiu, 1996).

The position of the lacrimal foramen (outside the orbit) was partly the reason for Mein and Ginsburg (2002) to place also intermediate- to large-sized material from La Grive (previously assigned to '*Amphechinus intermedius*') outside *Amphechinus*, and include it into *Postpalerinaceus*, a genus initially erected as a subgenus of '*Palerinaceus*' (junior synonym of *Amphechinus*) by Crusafont and De Villalta, 1947, but later upgraded to specific rank by Butler (1956) in order to accommodate large-sized material from the early late Miocene (MN10) of Spain. *Postpalerinaceus* was defined on a mix of both cranial and dental characters, and was considered (like *Mioechinus*) to occupy a morphologically intermediate position between a late Oligocene-early Miocene evolutionary stage (*Amphechinus*) and the modern stage (*Erinaceus*, *Atelerix*). Two other forms from la Grive, one of intermediate size and one of small size and both also with their lacrimal foramen outside the orbit, were placed by Mein and Ginsburg (2002) into the modern genus *Atelerix* as *A. depereti* and *A. rhodanicus*, respectively. Moreover, based on a comparison between palatal morphology in *Mioechinus oeningensis* and *Atelerix*, these authors proposed to include the genus *Mioechinus* into *Atelerix*. Other workers (e.g., Ziegler, 2005), however, consider palatal shape different enough to retain *Mioechinus* as a separate genus.

The Spanish Miocene mammal record is very rich in sites, of which a significant part has yielded Erinaceinae. However, as most of these sites contain only a few dental elements, in most cases generic assignments cannot be certain. The genus name *Amphechinus* was used by Gibert (1975) to accommodate teeth and mandibular parts from the middle and early late Miocene of the northeastern and eastern-central part of Spain. Whereas the oldest (MN5) material described by Gibert ('*A. baudeloti*') includes several small-sized, rectangularly shaped upper molars that resemble those considered to represent 'true' *Amphechinus* (e.g., as in Ziegler et al., 2007), the dentition of the middle Miocene (MN6) large-sized '*A. robinsoni*' is clearly more advanced, rather resembling that of forms such as *Mioechinus oeningensis*. Despite its small size, '*A. golpae*' (earliest MN9 species represented by a mandibular fragment with p4-m3) seems also relatively advanced, lacking the slenderness of molars and mandible that characterize the late Oligocene and early Miocene *Amphechinus*. Consistently, in their summary work on the middle Miocene small mammal record from the Calatayud-Montalbán Basin, Van der Meulen et al. (2012) prefer to refer to the erinaceine material of this period as *Amphechinus*.

Despite its old age, a small-sized maxillary fragment with P3-M3 from the Vallès-Penedès Basin (Sant Mamet, MN4, late early Miocene; Crusafont et al., 1955) was not assigned to *Amphechinus*, but to *Mioechinus* (*M. butleri*). This choice seems justified given its surprisingly modern ('molarized') dental habitus with similarly-sized and square-shaped P4, M1 and M2, and with a P3 with a well-developed lingual part (even containing a hypocone). As referred to above, there is also little doubt that *Postpalerinaceus vireti*, defined

in the same basin, represents a clearly advanced form with regard to *Amphechinus*. Recently, this large-sized form has also been recognized (with complete hemimandibles) outside its type area with a record in the Madrid Basin (Cerro de Batallones, MN10; Álvarez-Sierra et al., 2017). A possible occurrence in eastern Central Spain even during times as young as MN17 was previously hypothesized (Crochet and Heintz, 1971).

In this paper we summarize the erinaceine remains as recovered from the dense late Miocene micromammal sequence from the Teruel Basin (Fig. 1). The record consists of 123 dental elements originating from 28 localities. For basin stratigraphy and chronology, we refer to Mein et al. (1990); Opdyke et al. (1997), and Van Dam et al. (2001, 2006, ongoing work). We also discuss some material from the neighboring Calatayud-Montalbán Basin, part of which is published (Cañada 6 and 12; López-Guerrero et al., 2011) and part of which has remained unpublished (Pedregueras 2C; for geographic and updated stratigraphic context, see Van Dam et al., 2014). We have assigned the studied material to the genera *Postpalerinaceus* and *Atelerix*, although these attributions should be considered as provisional given the need for a thorough revision of European Mio-Pliocene Erinaceinae (in which cranial characteristics may or may not play a role).

We will end our paper with a discussion on the temporal distribution of Iberian and European spiny hedgehogs. Their

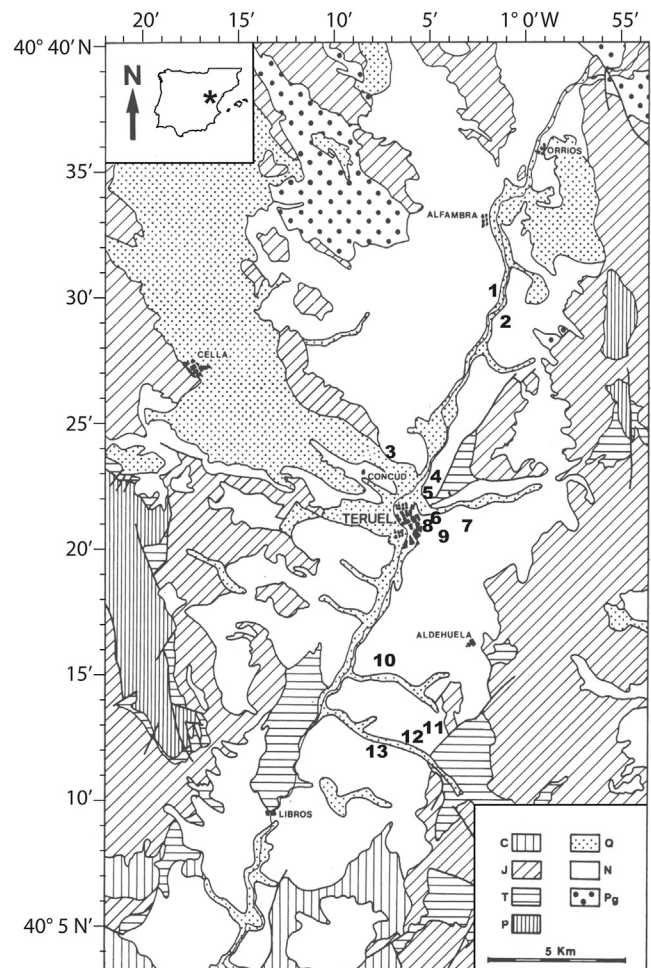


Fig. 1. MN10-13 sites in the Teruel Basin with Erinaceinae. 1: Masía de La Roma 3-4B-5-7-11; 2: Peralejos D; 3: Conclud Cerro de La Garita, Conclud 3; 4: Masada del Valle 2, Tortajada A, Masada Rueda 2-3; 5: Puente Minero, Puente Minero 2, Masía del Barbo 2A-2B; 6: Vivero de Pinos; 7: Los Aguanaces, Los Aguanaces 1-3, La Gloria 5-10-11; 8: Los Mansuetos; 9: Aljezar B; 10: Prado 3, 15C; 11: Cascante-Cubla 1; 12: Cascante 7A; 13: Patrimonio Forestal 5A.

middle to late Miocene radiation will be explained in terms of diet-related morphological change that was ultimately rooted in a basic Oligocene masticatory apparatus aimed at consuming small invertebrates. Finally, we invoke climatic cooling as a main cause for the remarkably low erinaceine abundance that characterizes the latest Miocene and Pliocene of both Spain and Europe as a whole.

2. Material and methods

The locations of the studied sites are shown in Fig. 1. The stratigraphic context and general fauna have been described elsewhere (e.g., Van de Weerd, 1976; Adrover, 1986; Mein et al., 1990; Van Dam et al., 2001) or their description is in progress (sites Concul Cerro de la Garita, Cascante 7A, Patrimonio Forestal 5A). The bulk of the studied material is housed in the collections of the Department of Earth Sciences of Utrecht University, Netherlands, the Museo Aragonés de Paleontología (Teruel, Spain), and the Collections de Géologie of the Centre de Ressources pour les Sciences de l'Evolution, Université Claude Bernard (Lyon, France). Tables 1–4 contain the complete list of the studied material. Summaries with element types and left/right assignments are included in the systematic part below (Section 4). This study essentially contains all upper Miocene erinaceine material from the Teruel Basin known so far, except for material from Aljezar B (MN12). This material, described as *Erinaceus* sp. (Adrover, 1986; Van den Hoek Ostende and Furió, 2005) could not be recovered and could therefore not be included in this study.

During our investigation, we have compared our material with the type material of key species from the Iberian Peninsula, including *Mioechinus butleri*, *Amphechinus robinsoni* (Manchones) and *Postpalerinaceus vireti* (Viladecaballs, Can Llobateres, and Can Ponsic) stored in the Institut Català de Paleontologia Miquel Crusafont (ICP) and in the Utrecht and Lyon collections. Part of the specimens encountered in the ICP collection were re-measured. Furthermore, we compared our specimens to the literature descriptions and figures from relevant Spanish and French

populations (notably Crusafont and De Villalta, 1947; Crusafont and Gibert, 1974; Engesser, 2009; Gibert, 1975; Mein and Ginsburg, 2002; Viret, 1938). Finally, tooth rows of modern European and African taxa (*Erinaceus*, *Atelerix*) were used for comparison (both museum material and published photographs, e.g., Gould, 2001).

The measurement method for molars and p4/d4 follows De Jong (1988). For the incisors, canine, premolars (except for P4) and deciduous teeth, length was measured as the maximum longitudinal distance, and width by taking it perpendicularly to it. In their description of the Erinaceinae from La Grive (included in our discussion), Mein and Ginsburg (2002) use the measurement method of Mein and Martín-Suárez (1994) as used for Galericiini (the other main subfamily of Erinaceidae). Because of the symmetrical shape of the P3 of Erinaceinae, both measurement methods will yield almost equal results for this element. Comparisons between P4s, however, require additional care, due to the use of a different method. Although the Teruel Basin contains very few P4 (only two fragments), the effect of the method is still relevant here, as also material from other regions will be discussed. Differences in length and width measurement of the P4 may stem from the fact that Mein and Martín-Suárez (1994) base their enclosing L-W rectangle on an anteriorly placed reference line (touching the outline at the level of both protocone and metacone), whereas De Jong (1988) places his reference line along the buccal border, which is obliquely positioned with regard to the anterior border in most Erinaceinae. Unfortunately, several of the older relevant publications of Spanish material (Crusafont and de Villalta, 1974; Crusafont and Gibert, 1974; Gibert, 1975) lack a clear description of how length and width are measured in the upper premolars. On the other hand, Crusafont et al. (1955) mention that P4 length was measured along the buccal border (*Mioechinus butleri*). We assume that length was measured similarly in the later papers by Crusafont, Gibert and colleagues, and that width was measured perpendicular to length (essentially De Jong's method). The scatter for P4 as included in this paper should nevertheless be judged with care, as L and W for French (La

Table 1

Studied material of *Postpalerinaceus* cf. *vireti* and measurements. Specimens from the Lyon collection are without individual catalogue numbers. Measurement method for molars, p4 and P3 after De Jong (1988), and for P4 after Mein and Martín Suárez (1994). Length for incisors, canines, P2 and p3 taken maximally, and width taken perpendicular to length.

Locality	Code	MN	Local Zone	Age (Ma)	Sup./Inf.	Element type	Element nb.	Dex./Sin.	Storage	Catalogue nb.	Length (mm)	Width (mm)
La Gloria 10	GLO10	11	K	8.4	sup.	i	1	dex.	UU(MAP)	381		
Los Aguanaces 1	AG1	11	K	8.4	sup.	di	2	sin.	UU(MAP)	320	2.00	1.46
Masía del Barbo 2A	MB2A	10	J1	9.8	sup.	di	2	dex.	UU	1129	1.36	1.37
Vivero de Pinos	VIP	11	K	8.2	sup.	di	2	dex.	LY		1.40	1.44
La Gloria 10	GLO10	11	K	8.4	sup.	di	2	dex.	UU	382	1.70	1.53
La Gloria 11	GLO11	11	J4	8.8	sup.	i	2	sin.	UU	56	2.03	1.70
Masía de la Roma 3	ROM3	9	I	10.1	sup.	i	2	dex.	UU(MAP)	304	2.08	1.60
Masía del Barbo 2A	MB2A	10	K	9.8	sup.	c	1	sin.	UU	1130		1.30
Los Aguanaces 3	AG3	11	K	8.2	sup.	p	2	sin.	UU(MAP)	2109	2.16	1.90
Vivero de Pinos	VIP	11	K	8.2	sup.	p	2	dex.	LY		2.39	1.92
Masía del Barbo 2B	MBB	10	J2	9.7	sup.	p	2	sin.	UU	2058	1.98	1.85
Los Aguanaces	AG	11	K	8.2	sup.	m	2	dex.	LY		4.77	5.42
Peralejos D	PERD	11	J4	8.8	inf.	i	3	sin.	UU(MAP)	630		1.70
Masía del Barbo 2B	MB2B	10	J2	9.7	inf.	i	3	sin.	UU	2055	2.26	1.71
La Gloria 10	GLO10	11	K	8.4	inf.	c	1	sin.	UU(MAP)	384	3.29	2.05
La Gloria 10	GLO10	11	K	8.4	inf.	c	1	sin.	UU(MAP)	385	3.22	2.11
La Gloria 10	GLO10	11	K	8.4	inf.	p	3	sin.	UU(MAP)	386	2.15	1.83
La Gloria 10	GLO10	11	K	8.4	inf.	p	3	sin.	UU(MAP)	387		
Vivero de Pinos	VIP	11	K	8.2	inf.	p	3	dex.	LY		1.75	1.53
Vivero de Pinos	VIP	11	K	8.2	inf.	p	3	dex.	LY		1.93	1.90
Vivero de Pinos	VIP	11	K	8.2	inf.	p	3	dex.	LY		2.06	1.77
Cascante-Cubla 1	CCUB1	11	J4	8.8	inf.	p	4	sin.	LY			
Masía del Barbo 2B	MB2B	10	J2	9.7	inf.	m	1	sin.	UU	2056		
Masía del Barbo 2B	MB2B	10	J2	9.7	inf.	m	1	sin.	UU	2057		
Masía del Barbo 2B	MB2B	10	J2	9.7	inf.	m	1	dex.	UU	2059	5.86	3.54

Table 2
Studied material of *Atelexer* aff. *depereti* and measurements. See Table 1 for measuring details.

Locality	Code	MN	Local Zone	Age (Ma)	Sup./Inf.	Element type	Element nb.	Dex./Sin.	Storage	Catalogue nb.	Length (mm)	Width (mm)
Los Aguanaces 3	AG3	11	K	8.2	sup.	i	1	sin.	UU(MAP)	2101	1.80	
Vivero de Pinos	VIP	11	K	8.2	sup.	i	1	dex.	LY		1.96	1.48
Masada Rueda 2	MRU2	11	K	8.5	sup.	i	1	dex.	MAP	189	1.28	
Masía de la Roma 5	ROM5	10	J1	9.9	sup.	i	1	sin.	UU(MAP)	21	1.88	
Masía de la Roma 7	ROM7	10	J1	9.8	sup.	i	2	dex.	UU(MAP)	259	1.40	1.04
Concud Cerro de la Garita	CG	12	L	7.5	sup.	i	3	dex.	MAP	754	1.73	1.47
Los Aguanaces 3	AG3	11	K	8.2	sup.	i	3	dex.	UU(MAP)	2114		
Los Aguanaces 3	AG3	11	K	8.2	sup.	i	3	dex.	UU(MAP)	2108	2.30	1.75
Vivero de Pinos	VIP	11	K	8.2	sup.	i	3	dex.	LY		2.24	1.85
Masía de la Roma 11	ROM11	10	J2	9.5	sup.	i	3	sin.	UU(MAP)	310		
Los Mansuetos	LM	12	L	7.3	sup.	c	1	sin.	MAP	4005	2.42	1.67
Vivero de Pinos	VIP	11	K	8.2	sup.	c	1	dex.	LY		1.77	1.62
Vivero de Pinos	VIP	11	K	8.2	sup.	c	1	sin.	LY		1.99	1.67
Prado 15C	PRD15C	10	J1	9.8	sup.	c	1	sin.	MAP	186	2.67	1.70
Masía de la Roma 3	ROM3	9	I	10.1	sup.	c	1	sin.	UU(MAP)	306		
Masía de la Roma 3	ROM3	9	I	10.1	sup.	c	1	sin.	UU(MAP)	307		
Los Aguanaces 3	AG3	11	K	8.2	sup.	p	2	dex.	UU(MAP)	2112	2.21	1.72
Los Aguanaces 3	AG3	11	K	8.2	sup.	p	2	dex.	UU(MAP)	2113	2.07	1.59
La Gloria 10	GLO10	11	K	8.4	sup.	p	2	dex.	UU(MAP)	383	2.41	1.75
La Gloria 10	GLO10	11	K	8.4	sup.	p	2	sin.	UU(MAP)	388		
La Gloria 10	GLO10	11	K	8.4	sup.	p	2	dex.	UU(MAP)	389		
Prado 3	PRD3	10	J1	9.7	sup.	p	2	sin.	MAP	189	1.87	1.54
Vivero de Pinos	VIP	11	K	8.2	sup.	dp	3	sin.	LY		2.10	1.58
Vivero de Pinos	VIP	11	K	8.2	sup.	dp	3	sin.	LY		1.97	1.50
Vivero de Pinos	VIP	11	K	8.2	sup.	dp	3	sin.	LY		1.80	1.21
Los Aguanaces	AG	11	K	8.2	sup.	p	3	dex.	LY		2.08	2.32
Vivero de Pinos	VIP	11	K	8.2	sup.	p	3	sin.	LY		2.38	3.05
Pedregueras 2C	PED2C	9	I	10.4	sup.	p	3	dex.	UU	1311	1.98	2.27
Los Aguanaces	AG	11	K	8.2	sup.	p	4	dex.	LY		4.41	
Masía de la Roma 11	ROM11	10	K	9.5	sup.	p	4	dex.	UU(MAP)	309		
Los Aguanaces	AG	11	K	8.2	sup.	m	1	dex.	LY		4.91	5.57
Vivero de Pinos	VIP	11	K	8.2	sup.	m	1	dex.	LY		4.90	5.10
Puente Minero	PM	11	K	8.4	sup.	m	1	dex.	MA	1753	5.5*	5.6*
Los Mansuetos	LM	12	L	7.3	sup.	m	2	dex.	UU	4001		
Los Mansuetos	LM	12	L	7.3	sup.	m	2	sin.	UU	4002	3.90	4.62
Los Aguanaces	AG	11	K	8.2	sup.	m	2	dex.	LY		4.27	4.90
Vivero de Pinos	VIP	11	K	8.2	sup.	m	2	sin.	LY		4.45	4.90
Prado 15C	PRD15C	10	J1	9.8	sup.	m	2	dex.	MAP	190		
Pedregueras 2C	PED2C	9	I	10.4	sup.	m	2	dex.	UU	1312		
Tortajada A	TOA	11	K	8.2	sup.	m	3	dex.	UU	2001	1.69	3.17
Vivero de Pinos	VIP	11	K	8.2	sup.	m	3	sin.	LY		1.61	2.95
Vivero de Pinos	VIP	11	K	8.2	sup.	m	3	sin.	LY		1.69	3.06
Masía de la Roma 7	ROM7	10	J1	9.8	sup.	m	3	dex.	UU(MAP)	260	1.67	2.86
Masía de la Roma 3	ROM3	10	I	10.1	sup.	m	3	dex.	UU(MAP)	301	1.60	2.87
Concud 3	CC3	12	L	7.2	inf.	i	3	sin.	UU	3016	1.81	1.36
Concud 3	CC3	12	L	7.2	inf.	i	3	dex.	UU	3017	2.04	1.59
Concud 3	CC3	12	L	7.2	inf.	i	3	sin.	UU	3018	2.02	1.62
Los Aguanaces 3	AG3	11	L	8.2	inf.	i	3	sin.	UU(MAP)	2110	2.46	
Vivero de Pinos	VIP	11	K	8.2	inf.	i	3	sin.	LY		1.77	1.62
Masía del Barbo 2A	MB2A	10	J1	9.8	inf.	i	3	dex.	UU	2084	2.01	1.56
Masía de la Roma 9	ROM9	10	J1	9.8	inf.	i	3	sin.	UU(MAP)	158	1.98	
Cascante 7A	CASC7A	10	J1	9.5	inf.	c	1	sin.	MAP	9		
Prado 15C	PRD15C	10	J1	9.8	inf.	c	1	sin.	MAP	185		1.54
Prado 15C	PRD15C	10	J1	9.8	inf.	c	1	sin.	MAP	187	2.46	1.71
Masía de la Roma 3	ROM3	9	I	10.1	inf.	c	1	dex.	UU(MAP)	302	2.37	1.55
Concud 3	CC3	12	L	7.2	inf.	p	3	dex.	UU	3030	2.02	1.39
Concud Cerro de la Garita	CG	12	L	7.5	inf.	p	3	sin.	MAP	755	2.04	1.63
Concud Cerro de la Garita	CG	12	L	7.5	inf.	p	3	dex.	MAP	756	1.63	1.63
Masía del Barbo 2B	MB2B	10	J2	9.7	inf.	p	3	dex.	UU	2052	2.04	1.64
Masía del Barbo 2A	MB2A	10	J1	9.8	inf.	p	3	dex.	UU	2083	1.92	1.85
Los Aguanaces 3	AG3	11	K	8.2	inf.	p	4	dex.	UU(MAP)	2111		
Vivero de Pinos	VIP	11	K	8.2	inf.	p	4	sin.	UU(MAP)	803		
Vivero de Pinos	VIP	11	K	8.2	inf.	p	4	dex.	LY		2.49	1.81
Prado 3	PRD3	10	J1	9.7	inf.	p	4	sin.	MAP	188		
Puente Minero 2	PM2	10	J2	9.7	inf.	p	4	dex.	UU(MAP)	202		
Vivero de Pinos	VIP	11	K	8.2	inf.	m	1	sin.	LY			
Concud Cerro de la Garita	CG	12	L	7.5	inf.	m	2	sin.	MAP	751		
Concud Cerro de la Garita	CG	12	L	7.5	inf.	m	2	sin.	MAP	752	5.00	2.99
Vivero de Pinos	VIP	11	K	8.2	inf.	m	2	sin.	UU(MAP)	802		
Vivero de Pinos	VIP	11	K	8.2	inf.	m	2	sin.	LY		4.84	3.43
La Gloria 5	GLO5	13	M2	6.4	inf.	m	3	dex.	LY		1.98	1.62
Concud Cerro de la Garita	CG	12	L	7.5	inf.	m	3	dex.	MAP	753	2.01	1.60

Table 2 (Continued)

Locality	Code	MN	Local Zone	Age (Ma)	Sup./Inf.	Element type	Element nb.	Dex./Sin.	Storage	Catalogue nb.	Length (mm)	Width (mm)
Vivero de Pinos	VIP	11	K	8.2	inf.	m	3	dex.	LY		2.31	1.84
Vivero de Pinos	VIP	11	K	8.2	inf.	m	3	dex.	LY		2.43	2.17
Prado 15C	PRD15C	10	J1	9.8	inf.	m	3	dex.	MAP	3	2.26	1.64
Pedregueras 2C	PED2C	9	I	10.4	inf.	m	123	dex.	UU	1314		

* Size extrapolation based on Alcalá et al. (1991: pl. 1, fig. 38).

Table 3

Studied material of *Aterix steensmai* nov. sp. and measurements. See Table 1 for measuring details.

Locality	Code	MN	Local Zone	Age (Ma)	Sup./Inf.	Element type	Element nb.	Dex./Sin.	Storage	Catalogue nb.	Length (mm)	Width (mm)
Masada del Valle 2	MDV2	12	L	7.6	sup.	i	2	sin.	UU	4051	2.40	1.59
Masada del Valle 2	MDV2	12	L	7.6	sup.	c	1	dex.	UU	4067	3.64	2.03
Masada Ruea 3	MRU3	12	L	7.5	sup.	p	2	sin.	MAP	364	2.71	2.02
Masada del Valle 2	MDV2	12	L	7.6	sup.	p	2	dex.	UU	4068	2.70	2.06
Masada del Valle 2	MDV2	12	L	7.6	sup.	m	1	dex.	UU	4074		
Masada del Valle 2	MDV2	12	L	7.6	sup.	m	1	dex.	UU	4075		
Masada del Valle 2	MDV2	12	L	7.6	sup.	m	2	dex.	UU	4072	4.59	5.27
Masada del Valle 2	MDV2	12	L	7.6	inf.	i	3	dex.	UU	4054	2.86	2.01
Masada del Valle 2	MDV2	12	L	7.6	inf.	i	3	dex.	UU	4055		1.97
Masada del Valle 2	MDV2	12	L	7.6	inf.	c	1	sin.	UU	4066	3.63	2.00
Masada Ruea 3	MRU3	12	L	7.5	inf.	p	4	sin.	MAP	363		
Masada del Valle 2	MDV2	12	L	7.6	inf.	p	4	sin.	UU	4064		
Masada del Valle 2	MDV2	12	L	7.6	inf.	m	1	sin.	UU	4071		
Masada Ruea 3	MRU3	12	L	7.5	inf.	m	2	dex.	MAP	231	5.04	3.82
Masada del Valle 2	MDV2	12	L	7.6	inf.	m	2	dex.	UU	4061	5.70	3.80
Masada del Valle 2	MDV2	12	L	7.6	inf.	m	2	sin.	UU	4076		
Masada del Valle 2	MDV2	12	L	7.6	inf.	m	2	sin.	UU	4077		

Table 4

Studied material of Erinaceinae indet. and measurements. See Table 1 for measuring details.

Locality	Code	MN	Local Zone	Age (Ma)	Sup./Inf.	Element type	Element nb.	Dex./Sin.	Storage	Catalogue nb.	Length (mm)	Width (mm)
Los Aguanaces 3	AG3	11	K	8.2	sup.	i	2	sin.	UU(MAP)	2102	1.73	1.13
Los Aguanaces 3	AG3	11	K	8.2	sup.	i	3	sin.	UU(MAP)	2103	2.22	1.72
Masía de la Roma 3	ROM3	9	I	10.1	sup.	m	2	dex.	UU(MAP)	308		
Los Aguanaces 3	AG3	11	K	8.2	sup.	m	3	dex.	UU(MAP)	2107	1.54	2.92
Patrimonio Forestal 5A	PF5A	11	J4	8.8	sup.	p	2	dex.	MAP	52		
Puente Minero 2	PM2	10	J2	9.7	sup.	p	4	sin.	UU(MAP)	201		

Grive) specimens will be somewhat under- or over-estimated, respectively, with regard to the Spanish specimens.

3. Dental variation

The classification of isolated fossil Erinaceinae teeth is partly hampered by the lack of sufficient comparative material. Especially variation in the anterior elements remains poorly known. Morphological convergence of posterior incisors, canine and anterior premolars is an additional complicating factor. The following paragraphs (which particularly focus on Miocene Erinaceinae from Europe) summarize our criteria for recognizing the different elements and for assigning these to the different genera.

The tooth formula of Erinaceinae is I 3/2 C 1/1 P 3/2 M 3/3, although an additional lower premolar is still present in primitive representatives (e.g., *Paleoscapter* from the Oligocene and lower Miocene of Asia; Ziegler et al., 2007). Anomalies in tooth number seem to be common. For instance, variability in tooth numbers is recorded in modern *Erinaceus europaeus* for the lower incisors and upper premolars. P3 may be missing entirely in this species (Reeve, 1994) and *Aterix* (e.g., in the type species *A. albiventris*; Santana

et al., 2010). Recently, the remarkable occurrence of a M4 was discovered in the living Asian species *Mesechinus wangi* (Ai et al., 2018).

3.1. Upper dentition

Upper erinaceine incisors have a convex external (buccal or antero-buccal) and concave internal (lingual or postero-lingual) side. I1 is the largest upper incisor. It is elongated, relatively curved, and usually has a sharp posterior edge. The single, long root of the I1 extends below the posterior incisors and may reach the level of C. I2 is the smallest of the three upper incisors. Its crown is relatively pointed and it has one root. Its crown base is curving upward in buccal direction. I3 is much larger and tends to be caniniform, with both faces separated by a relatively sharp, buccally placed longitudinal ridge. I3 tends to have a characteristic root positioning, with two parallel roots pointing backward with regard to an anteriorly up-curving crown base (e.g., *Mioechinus tobieni* in Engesser, 1980: figs. 22, 23). In some forms (e.g., modern *Aterix*) either one or two roots may occur (Gould, 2001). In rare instances where fossil DI2-3 where found, they generally resembled I2-3 (e.g., *P. intermedius* from La Grive; Mein and Ginsburg, 2002).

Compared to I and P, C is relatively symmetric bucco-lingually. It is dominated by a centrally positioned main cusp, from which a posterior crest and usually also an anterior crest are running downward. In the most primitive forms, the upper canine is larger and higher than I3 and P2. In the late Miocene *Postpalerinaceus vireti*, C is very large compared to the neighboring elements, with the main cusp positioned relatively anteriorly and the anterior part occupied by a high anterior shelf instead of a crest (observation on the holotype specimen). In contrast to the configuration in I3, the two roots tend to diverge. DC resembles C, but its main cusp tends to be situated at a more anterior position (for example *Postpalerinaceus intermedius*; Mein and Ginsburg, 2002: Fig. 5).

Generally, the P2 is small. Its occlusal outline varies between rounded and sub-rectangular. The P2 contains one, antero-buccally placed main cusp, which is lower than its homologous cusp in C and I3, and from where a buccal cutting edge is running in posterior direction. Normally, the P2 contains two slightly diverging roots, which may be fused (as in *A. edwardsi*, Viret, 1938) or incipiently fused (as in *P. intermedius*; Mein and Ginsburg, 2002). The stronger, posterior root is flattened. In various forms (e.g., *Mioechinus oeningensis*, *M. tobieni*; Engesser, 1980: fig. 24a,c) the postero-lingual part of the crown extends downward over the posterior root, creating a sub-rectangular outline in occlusal view and an apparently oblique position of the posterior root with regard to the posterior outline. A similar shape was described for *P. intermedius* from La Grive (site L3), whereas a more rounded shape was pictured for *Atelexis depereti* from the same site (Engesser, 1980: fig. 24b; '*M. sansaniensis*', later reassigned to *A. depereti* by Mein and Ginsburg, 2002). According to Mein and Ginsburg (2002), DP2 (*P. intermedius* from La Grive) more or less resembles P2.

P3 has a sub-triangular outline with a strong buccal part and a poorly developed lingual part. Its shape and size can be interpreted as strongly reduced with respect to P4. The lingual part may sometimes be well developed as in modern *Erinaceus*, in which its shape nevertheless tends to be highly variable (Reeve, 1994), but also in old forms such as *Mioechinus butleri*, where it even contains a hypocone (Crusafont et al., 1955). Length exceeds width in *M. tobieni* and *Atelexis depereti* (Engesser, 1980; Mein and Ginsburg, 2002), but the reverse is true for *P. vireti* (type material; Crusafont and De Villalta, 1947). Mostly three roots have been observed. Where encountered (e.g., *P. intermedius*, La Grive), DP3 are highly variable in shape, with the lingual parts more poorly developed than in P3.

P4 is a genuine carnassial tooth and easy recognizable by its high and sharp buccal cutting edge. This edge may be quite long, causing the outline to become trapezium-shaped (e.g., in the primitive *A. edwardsi*; Viret, 1938). The degree of molarization in the P4 is still low in *M. tobieni* (small-sized, lingual length reduced), but is larger in *M. oeningensis* and *A. depereti*. By contrast, molarization is well advanced in forms such as *M. butleri*, *P. intermedius* (e.g., Engesser, 2009) and *Erinaceus*, in which the P4 is almost square-shaped. The P4 has three roots. Compared to P4, DP4 has its lingual part reduced.

M1 has a rectangular outline in most of the older early-middle Miocene forms (*Amphechinus*, *Postpalerinaceus intermedius*), whereas a square shape is common in younger forms (*P. vireti*, *Atelexis*, *Erinaceus*). An exception to this trend is formed by the late early Miocene *Mioechinus butleri*, which shows square-shaped M1, M2 and P4 that are similarly sized. Generally, however, M1 size clearly exceeds that of P4 and M2 in most older forms, whereas the three teeth have a similar size in modern forms (e.g., *Erinaceus*). The metastyle in M1 is usually stronger than the parastyle (exception: *M. oeningensis*). The metastyle may sometimes be very pronounced, for instance in the rectangular shaped, 'premolarized' M1 of '*Amphechinus*' *baudeloti* (Gibert, 1975). A metaconule is

typically present in M1, although it is presumably absent in the most primitive (latest Oligocene and earliest Miocene) *Amphechinus* forms (Gibert, 1975). The protoconule is often absent. If present, its expression is variable: e.g., relatively distinct in *P. intermedius* from La Grive (Mein and Ginsburg, 2002), but represented by a faint swelling only in the same species from Sansan (Engesser, 2009). The M1 has three roots.

The M2 has a posteriorly tapering outline, because of a much stronger parastyle compared to the metastyle. A metaconule is present in *Mioechinus tobieni*, *Amphechinus baudeloti*, *A. robinsoni*, poorly developed or absent in *P. intermedius*, and absent (i.e. integrated in the metaloph) in *P. cingulatus* and *Atelexis depereti*. If present, the metaconule is weaker than in M1. Crusafont and De Villalta, 1947 mention an isolated M2 with a metaconule in *P. vireti* from Viladecaballs. The M2 has three roots.

The M3 is an antero-posteriorly reduced element with an elongated outline, which is oval- or drop-shaped. The protocone is the largest cusp. The smaller paracone may take the shape of a ridge (e.g., *Atelexis depereti* from Sansan, Engesser, 2009). One root is present in *M. tobieni* and various species of *Amphechinus* (Butler, 1948), whereas two, fused roots are present in *Atelexis depereti* (Mein and Ginsburg, 2002; Engesser, 2009). A variable root pattern has been observed in *P. intermedius* from La Grive with either one or two (separate or fused) roots.

3.2. Lower dentition

The i2 is the lower counterpart of I1. It is chisel-like and less curved than the latter. The flattened internal side may reveal an oblique (anterior) occlusal/wear surface that reminds that of rodent lower incisors (Viret, 1938). Its strong root extends far backwards and may reach the level of the p4 (e.g., *Amphechinus*; Butler, 2010).

The i3 is small and premolariform. It may be very low-crowned (as in *P. intermedius*) or somewhat more rounded and higher-crowned (as in *P. vireti*). It contains a longitudinally elongated, antero-buccally placed main cusp, which is integrated into the main longitudinal ridge. One posteriorly pointing root is present.

The shape of the slightly larger c resembles that of i3, but its outline is more oval. It is also asymmetric with the main cusp placed antero-buccally. It may show a tendency for bulbousness. One strong, posteriorly pointing root is present that runs less obliquely than in i3. The size of the lower canine approaches that of p4 in *Amphechinus*/*Postpalerinaceus*, whereas it is much smaller than p4 in *Erinaceus* (Viret, 1938).

The first premolar is generally considered to be a p3 (but see Butler, 1948, 2010). It has the shape of a rounded triangle with a straight posterior border. A single posterior root is present, the direction of which is less oblique than in c and i3. The p4 is a slightly molarized tooth with a short talonid. The protoconid is large and sharp. The metaconid tends to be present in older forms (e.g., *Amphechinus arvernensis*), whereas it is either absent (as in *P. intermedius* from Sansan) or distinctly present in younger forms (for instance, it is observed on the holotype of *Postpalerinaceus vireti*). The protoconid is positioned perpendicularly to the lingual border (e.g., in *P. intermedius* and *P. vireti*) or directed posteriorly (for instance in *Amphechinus robinsoni* and *Atelexis depereti*). The d4 is very different from p4 in early forms such as *A. edwardsi*. In this species it is only slightly molarized and basically consists of a massive posteriorly flattened cone with a small, incipient paraconid (Viret, 1938). The d4 of *P. intermedius* lacks a talonid. Its anterior part contains a small but distinct paraconid and contains a tiny, incipient metaconid as well (Mein and Ginsburg, 2002). In *Erinaceus*, the shape of d4 resembles that of p4, but the talonid is shorter, the cusps are less sharp, the paraconid is much lower than the protoconid, and the metaconid is not distinct.

As in the upper dentition, the second lower molar is relatively reduced with regard to the first molar in *Amphechinus*, whereas the size of both elements tends to converge in more advanced erinaceines. The trigonid is longer than the talonid in the m1 in all species of *Postpalerinaceus*. In this genus, the proto-lophid tends to run perpendicular to the lingual border, whereas in other forms the metaconid tends to be positioned more forward than the protoconid. In contrast to m1, the trigonid in m2 is not elongated. The paralophid, which may fully incorporate the paraconid, extends along the lingual border, in extreme cases reaching the metaconid (*A. baudeloti*; Gibert, 1975), thus closing the trigonid. Both m1 and m2 have two roots. The m3 basically consists of a trigonid, and has one root.

4. Systematic paleontology

The systematic allocation of the studied teeth presented below is sometimes tentative. This is because elements are represented by one or several specimens only and because the variation in some elements is poorly known in the first place. For these reasons we preferred to have the description of each element immediately followed by a short comparison/discussion where appropriate, instead of presenting a complete description per species followed by general discussion. Specimens smaller than half a tooth are referred to as 'fragm.' (fragment) in the material lists.

Abbreviations: **LY:** Collections de Géologie, Centre de Ressources pour les Sciences de l'Evolution, Université Claude Bernard, Lyon, France; **MAP:** Museo Aragonés de Paleontología, Spain; **UU:** Department of Earth Sciences, Utrecht University, Netherlands; **UU(MAP):** Department of Earth Sciences, Utrecht University, to be deposited in Museo Aragonés de Paleontología.

Order Eulipotyphla Waddell, Okada et Hasegawa, 1999
 Family Erinaceidae Fischer, 1814
 Subfamily Erinaceinae, Fischer, 1814
 Genus *Postpalerinaceus* Crusafont et Villalta, 1947
Type species: *Palerinaceus (Postpalerinaceus) vireti* Crusafont et Villalta, 1947

Postpalerinaceus cf. *vireti* Crusafont et Villalta, 1947

Fig. 2(A, B, C1-2)

2001. Erinaceinae indet. - Van Dam et al., pro parte (specimens from Masía de la Roma 3, Masía del Barbo 2B).

2011. cf. *Postpalerinaceus* - López-Guerrera et al., pro parte (specimen from Cañada 12).

Material (see Table 1 for locality abbreviations): AG: 1 RM2; AG1: 1 L(D?)I2; AG3: 1 LP2; CCUB1: 1 Lp4; GLO10: 1 RI1, 1 RI2, 1 LP2 (fragm.), 1 RP2, 2 Lc, 1 Lp3, 1 Lp3 (fragm.), 1 fragm.; GLO11: 1 LI2; MB2A: 1 R(D?)I2, 1 LC; MB2B: 1 LP2, 1 Li3, 1 Lm1, 1 Lm1 (fragm.), 1Rm1; PERD: 1 Li3; ROM3: 1 RI2; VIP: 1 RI2, 1 RP2, 3 Rp3.

Measurements: see Table 1 and Figs. 3–6.

Description and comparison: An external part of a large incisor from La Gloria 10 (GLO10-381, MN11) compares well to the external face I1 on the holotype skull of *Postpalerinaceus vireti* from Viladecaballs (MN10). Both specimens show the same moderately degree of curvature.

Six I2/DI2 have rounded circumferences, are relatively symmetric, have a concave postero-lingual face, and one big, rounded root. The specimens from Masía de la Roma 3 (ROM3-304, MN9) and La Gloria 11 (GLO11-56, MN10) are relatively large, whereas the specimens from Masía del Barbo 2A (MBA-1129, MN10), La Gloria 10 (GLO10-382, MN11, Fig. 2(A)), Los Aguanaces 1 (AG1-320, MN11), and Vivero de Pinos (MN11) are smaller in size. ROM3-304 has a small, laterally placed cusplule at the base of each

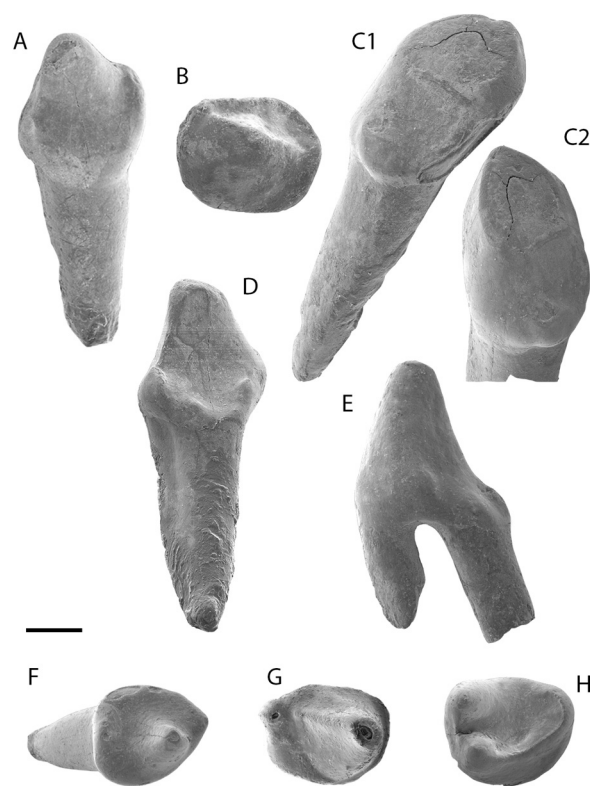


Fig. 2. A-C. *Postpalerinaceus* cf. *vireti* from various localities. A: right I2, GLO10-382; B: left i3, MBB-2055; C1: left c, GLO10-384, postero-lingual view; C2: left c, GLO10-384, postero-buccal view. D-H. *Atelerix* aff. *depereti* from various localities. D: right I3, AG3-2108; E: left C, LM-4005; F: left p3, CG-755; G: left P2, PRD3-189; H: right m3, CG-753. Scale bar: 1 mm.

of the two ridges that separate the convex from the concave face, whereas in GLO11-56 these additional cusplules seem to be lacking. MBA-1129 contains a relatively small and pointed main cusp and a broad basal rim. In this specimen, anterior and posterior ridges extend down from the pointed main cusp, with the posterior one being the sharpest. Very tiny additional cusplules occupy the ends of both ridges. A distinct, anteriorly climbing cingulum is present. Also GLO10-382 has a strong basal rim at the base of its concave face, although it is less pronounced. The La Gloria specimen has its root preserved, which is rounded, but somewhat flattened buccally. AG1-320 has a much weaker basal rim and an overall simpler shape. Similarly, the small specimen from VIP shows a simple, symmetric shape. Because of their smaller size, we tentatively assign the four latter specimens to DI2. In the type population of *P. intermedius* from La Grive a weaker cingulum was used as one of the features for separating I2 from DI2 (Mein and Ginsburg, 2002). Applied to our material, this criterion fits the identification of AG1-320 as a DI2, but would not fit our identification of the other two smaller-sized specimens.

The size of an anterior part of an upper canine (MBA-1130, MN10) implies a tooth size that is larger than that of *A. aff. depereti* (see below), fitting that of *P. vireti*. Its central cusp is rounded anteriorly and contains a faint and thin cingulum.

A complete P2 from La Gloria 10 (GLO10-383, MN11) has its main cusp worn flat. It lacks postero-central and lingual cusplules, but contains a very poorly developed postero-buccal cusplule. The lingual cingulum is restricted to the anterior part of the tooth. Another antero-buccal half of a P2 from the same site (GLO10-388) fits the morphology of the complete specimen.

A second premolar from Los Aguanaces 3 (AG3-2109, MN11) is larger than the other P2 from this site (identified below as *A. aff.*

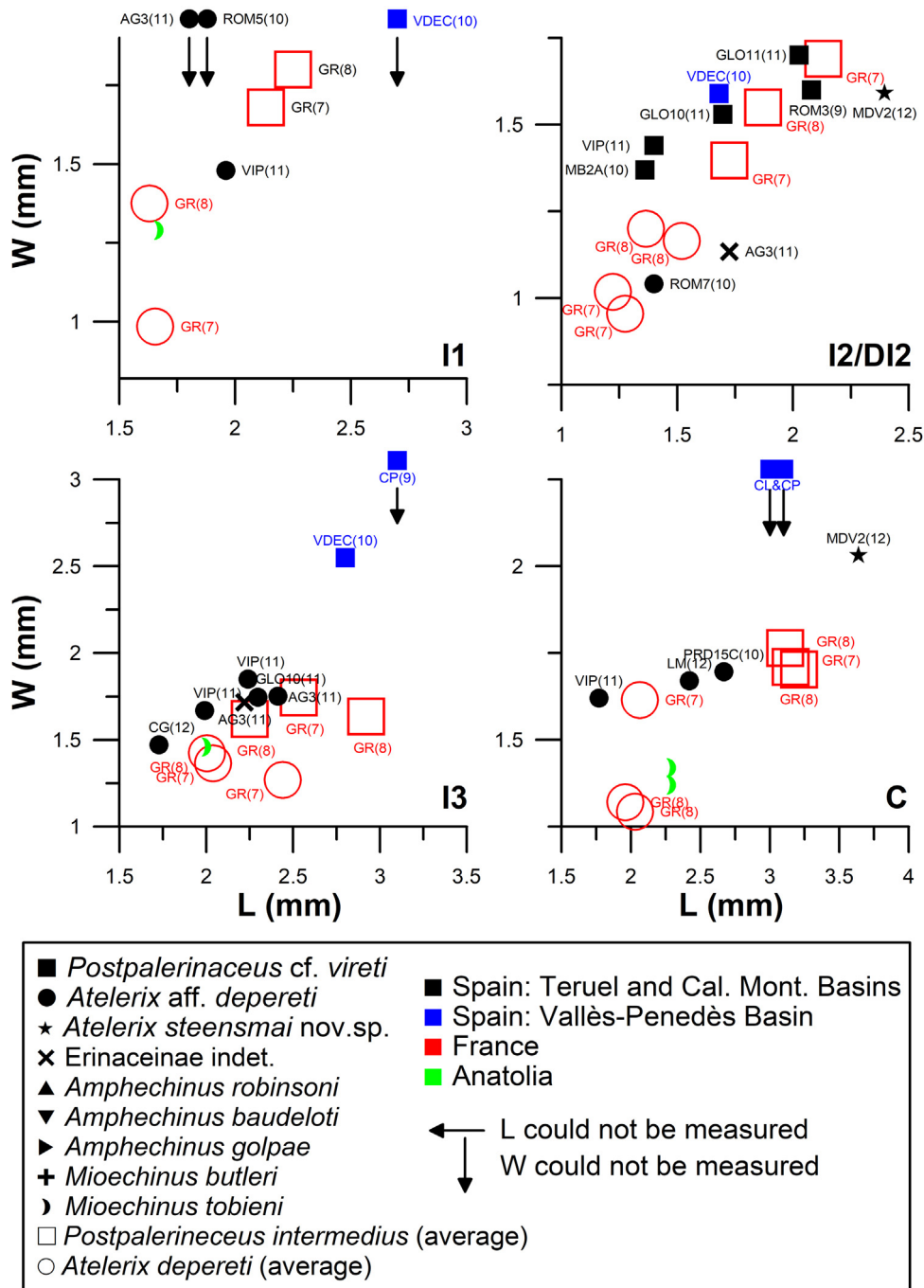


Fig. 3. Length-width scatters for I1, I2, I3, and C. See Tables 1–4 for L and W values.

depereti). Its shape is rounded and it is relatively broad. Its main cusp is pointing anteriorly, while its anterior face is sub-vertical. A postero-buccal shelf is present as well. The tooth contains at least two cuspules, which are placed postero-centrally and lingually on a weak cingulum. (The additional presence of a postero-lingual cuspule cannot be checked because of damage). A thin anterior cingulum is present. The broad posterior root is pointing downward (in contrast to I3, on which it would be directed more posteriorly). A specimen from Masía del Barbo 2B (MBB-2058, MN10) has a similar crown size and shape and posterior root shape. This specimen, which lacks the anterior part of its main cusp, has its posterior shelf less well developed than the specimen from Los Aguanaces 3.

Two M2 from Los Aguanaces (AG, MN11) clearly differ in size and morphology. In size, the largest of the two approaches the largest known specimen of *P. vireti* from its type area (Can Llobateres; Fig. 4). Because also the morphology of this specimen, with relatively straight borders and a lingual length that is distinctly smaller than its buccal length, is similar to that of the Can Llobateres specimen (as figured in Crusafont and Gibert, 1974), we are confident in assigning the larger of the two specimens from Los Aguanaces to *P. cf. vireti*.

The crown of i3 from Masía del Barbo 2B (MBB-2055, MN10; Fig. 2(B)) is not flat (as in *A. depereti*), but somewhat inflated. Its main cusp is part of a longitudinal ridge of which the height gradually decreases towards the posterior border, and which ends

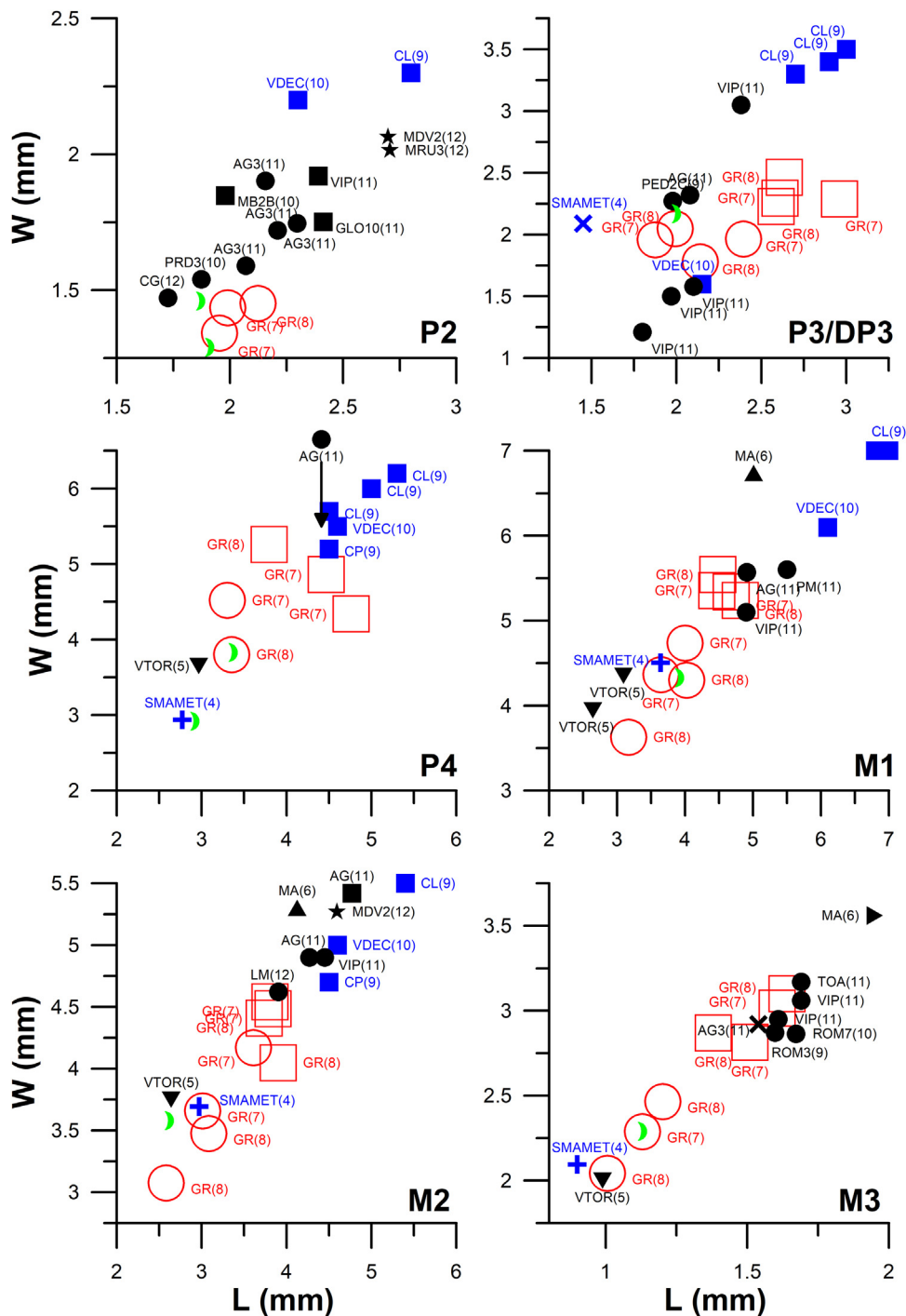


Fig. 4. Length-width scatters for P2, P3, P4, M1, M2, and M3. See Tables 1–4 for L and W values; see caption Fig. 3 for symbols.

in a posterior cuspule. Departing from this cuspule, a cingulum is running along the lingual border towards the anterior apex, from where it is climbing back towards the main cusp. The specimen resembles the i3 on the holotype of *P. vireti* from Viladecaballs, although it is somewhat smaller and lower-crowned. Unfortunately, the morphology of the lingual cingulum could not be compared to that of the holotype tooth, because the latter is both worn and damaged. The posteriorly damaged specimen from Peralejos D (PERD-630, MN11) is slightly less wide. It has a strong main cusp, which is included in a strong, antero-posteriorly running ridge.

Two lower canines from La Gloria 10 (GLO10-384 and 385, MN11; Fig. 2(C1,2)) are relatively bulbous. The anterior part of their occlusal surface is worn flat (as in P2). A small postero-buccal cuspule is present. The postero-lingual border is characterized by a low and broad cingulum ridge. Both teeth have very strong, backwards pointing roots.

A p3 from the same site (GLO10-386) has a rounded outline. It is wider anteriorly than posteriorly. The postero-lingual corner is the most reduced corner. The buccal border shows a little re-entrant between the larger anterior and smaller posterior part. A robust main cusp and a smaller posterior cusp are present, with no

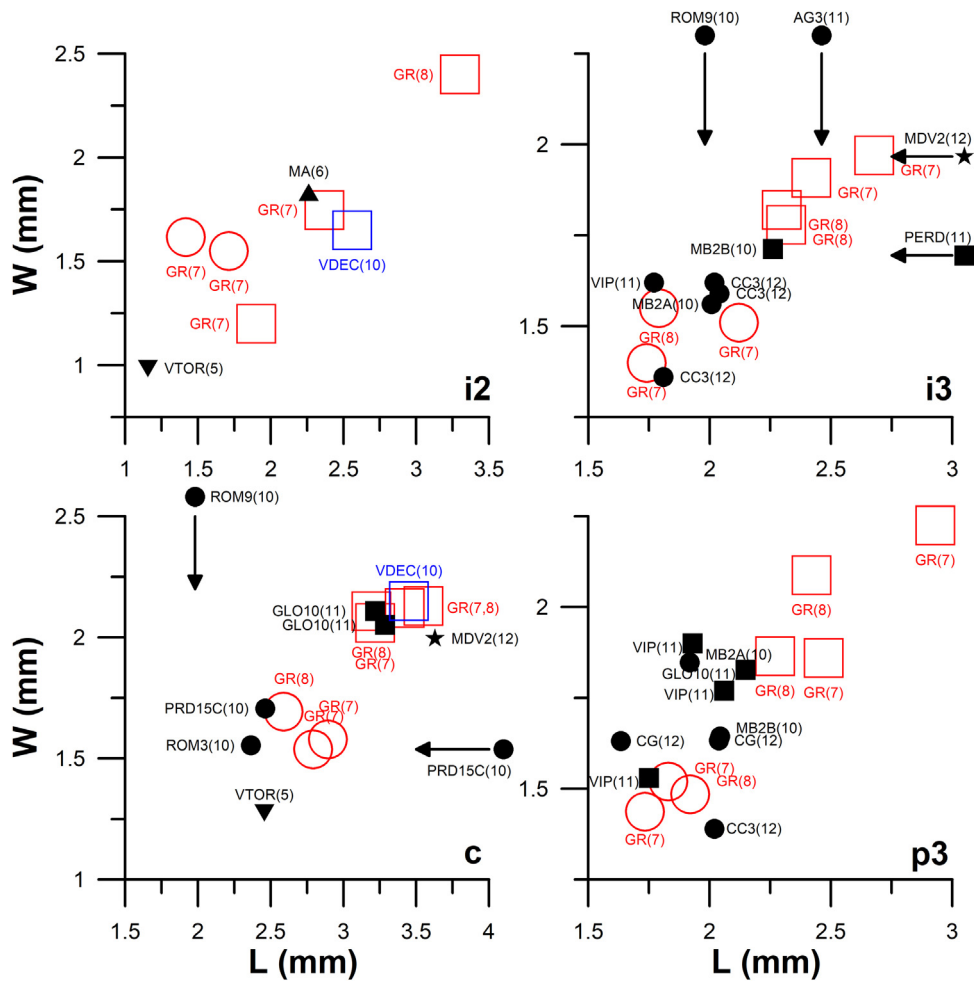


Fig. 5. Length-width scatters for i3, i3, c, and p3. See Tables 1–4 for L and W values; see caption Fig. 3 for symbols.

connecting ridge in between. The strong, posteriorly placed root is slightly curved posteriorly. An isolated posterior part from the same site (GLO-387) fits the morphology of the complete specimen. Three p3 from Vivero de Pinos have a similar rounded outline. Their root is straight, pointing slightly posteriorly.

The m1 from Masía del Barbo 2B (MBB-2059, MN10) has an elongated trigonid. The five main cusps have more or less equal heights, except for the hypoconid, which is somewhat lower. The protoconid-hypoconid and metaconid-entoconid connections are very thin and low. There is no sign of a posterior crest of the paraconid, leaving the central trigonid valley open lingually. The posterolophid ends freely against the entoconid, without contacting the posterior cingulum. This latter configuration also characterizes the talonid fragment MBB-2057. A strong posterior cingulum runs down from the entoconid, rounds the hypoconid and (in the complete MBB-2059) finally reaches the level of the paralophid. A fragment of a talonid from the same site (MBB-2056) with protoconid and metaconid present is assigned to *Postpalerinaceus* cf. *vireti* as well.

Genus *Aterlix* Pomel, 1848

Type species: *Erinaceus albiventris* Wagner, 1841

Aterlix aff. *depereti* Mein et Ginsburg, 2002

Figs. 2(D–H), 7(A–F), 8(I–J)

1986. *Postpalerinaceus vireti* - Adrover, pro parte (specimens from Los Aguanaces, Vivero de Pinos).

1992. *Amphichinus* cf. *robinsoni* - Alcalá et al.

2001. Erinaceinae indet. - Van Dam et al. (specimens from Masía de la Roma 7, Conclud 3 and Los Mansuetos).

2001. Erinaceinae indet. - Van Dam et al., pro parte (specimens from Masía de la Roma 3, Masía del Barbo 2B).

Material (see Table 2 for locality abbreviations): AG: 1 RP3, 1 RP4, 1 RM1, 1 RM2; AG3: 1 LI1, 2 RI3, 1 LP2, 2 RP2, 1 Li3, 1 Rm1 (fragm.); CC3: 2 Li3, 1 Ri3, 1 Rp3; CG: 1 RI3, GLO5: 1Rm3; LM: 1 LC, 1 LM2, 1 RM2; MB2A: 1 Ri3, 1 Rp3; MB2B: 1Rp3; MRU2: R1; PED2C: 1RP3, 1RM2 (fragm.), 1 fragm.; PM: 1RM1; PM2: 1Rp4; PRD3: 1LP2, 1Lp4 (fragm.), 1 fragm.; PRD15C: 1LC, 1RM2 (fragm.), 2 Lc, 1 Rm3; ROM3: 2 LC (fragm.), 1 RM3, 1Rc; ROM5: 1 LI1; ROM7: 1 RI2, 1 RM3; ROM9: 1 Li3; ROM11: 1 LI3, 1 RP4 (fragm.); TOA: 1RM3; VIP: 1 RI1, 1 RI3, 1 LC, 1 RC, 1 LP3, 2 LDP3, 1 RDP3, 1 RM1, 1 LM2, 2 LM3, 1 Li3, 1 Lp4, 1 Rp4, 1 Lm1, 2 Lm2, 2 Rm3.

Measurements: see Table 2 and Figs. 3–6.

Description and comparison: An external half of an I1 from Los Aguanaces 3 (AG3-2101, MN11; Fig. 7(F)) has a curved shape. The transition to the root is interrupted due to a cingulum-like extension at the base of the postero-lingual edge. The curvature is stronger than in the I1 from La Gloria 10 assigned to *Postpalerinaceus* cf. *vireti* (see above), and on the holotype from the latter species from Viladecaballs, which also is distinctly longer (2.7 mm). The length of the AG3 specimen (1.80 mm) is intermediate between that of *Aterlix depereti* (1.6–1.7 mm) and *P. intermedius* (2.0–2.3 mm) from la Grive. Because the figured I1 crown from La Grive (Mein and Ginsburg, 2002: fig. 4) lacks a basal

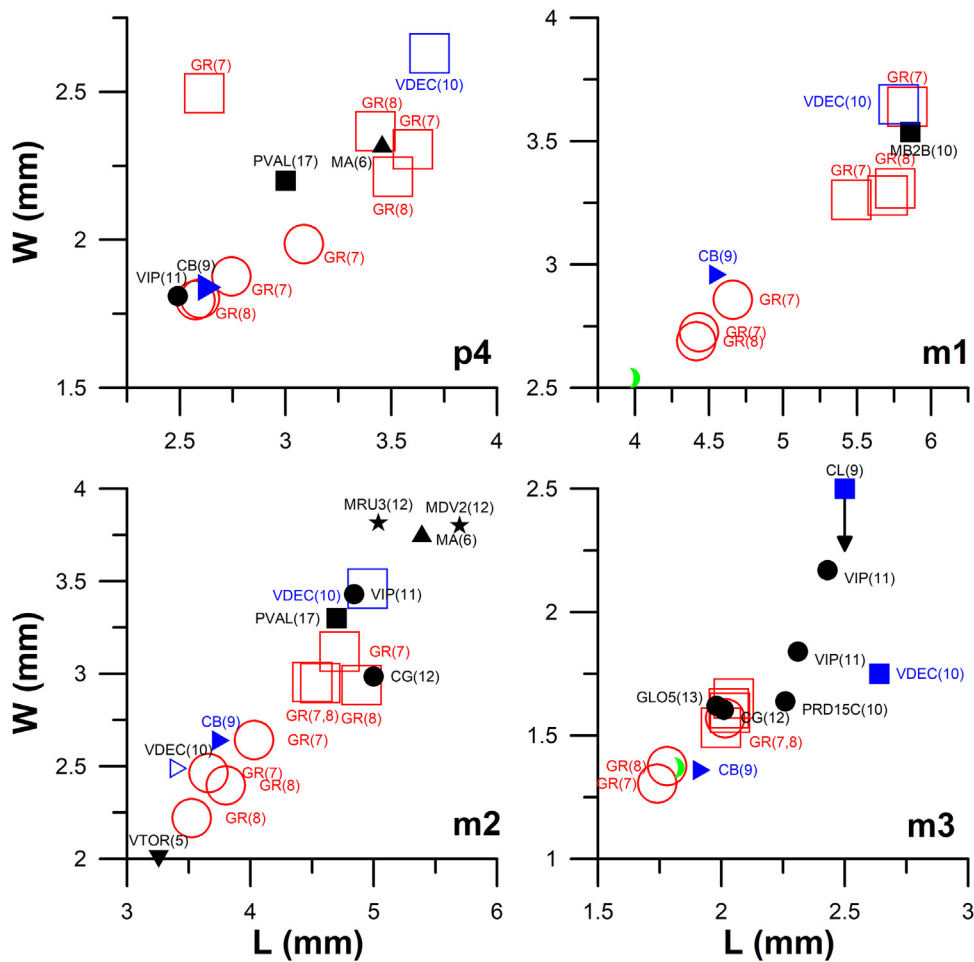


Fig. 6. Length-width scatters for p4, m1, m2, and m3. See Tables 1–4 for L and W values; see caption Fig. 3 for symbols.

posterior cuspule, we tentatively assign AG3-2101 to *A. aff. depereti*. An I1 from VIP (L=1.96 mm) also shows a postero-lingual extension at its base. A buccal part of an incisor (MRU2-189, MN11) is similarly shaped as the one from AG3-2101. A similarly sized (L=1.88 mm) buccal fragment from Masía de la Roma 7 (ROM5-21, MN10) is tentatively attributed to *A. aff. depereti* as well.

A small-sized I2 from Masía de la Roma 7 (ROM7-259, MN10; Fig. 7(E)) has a strongly flattened crown with a short anterior face and elongated posterior face. The lingual side is concave and the

buccal side is convex. Its main cusp is pointed. The lingual face is bounded by a relatively weak cingulum, which smoothly transforms into a climbing ridge that runs anteriorly and climbs upward towards the main apex. Another ridge that separates buccal from lingual face runs down posteriorly from the apex, and meets with the lingual cingulum. In contrast to the configuration in *Postpalerinaceus cf. vireti*, the single root is antero-posteriorly flattened with a curvature that mirrors that of the crown. The shape conforms to the description of I2 from *A. depereti* from La Grive, on which a strong antero-posterior asymmetry has been observed.

Three I3 were recovered from Los Aguanaces 3 (MN11; Fig. 2(D)). Their crowns contain a strong, antero-buccally placed pointed cusp, from which a pronounced ridge is descending along the buccal border, thereby creating a distinct cutting blade with a steep postero-lingual wall. This ridge ends in a postero-buccal cuspule. In one of the three specimens (AG3-2109) a postero-central cuspule is present as well. This cuspule is positioned on a faintly visible cingulum, which continues along the lingual side, reaching the level of the main cusp. A strong, antero-posteriorly flattened posterior root is preserved in AG3-2108. AG3-2114 is a postero-lingual part that is relatively unworn, containing a very pointed apex. A buccal fragment from Masía de la Roma 11 (ROM11-310, MN10) contains a main cusp from which a sharp ridge is descending buccally, ending in a small postero-buccal cuspule. All specimens have at least onsets of the posterior root preserved. This root is antero-posteriorly flattened and stands out at an oblique angle (~45°) with regard to the crown base. AG3-2108 and another specimen from Vivero de Pinos (VIP, MN11) also

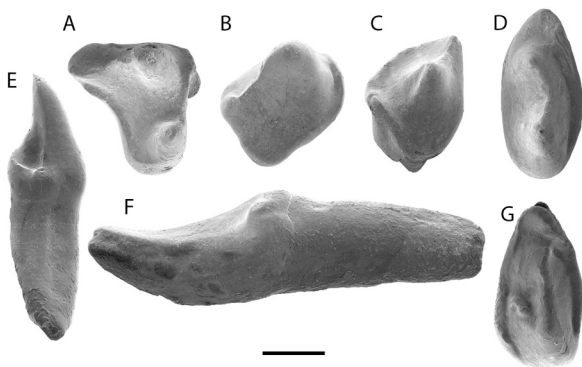


Fig. 7. A–F. *Atelerix aff. depereti* from various localities. A: right P3, PED2C-1311; B: right P2, AG3-2112; C: right p3, MBA-2083; D: right M3, ROM7-260; E: right I2, ROM7-259; F: right I1, AG3-2101. G. Erinaceinae genus and species indet. from Los Aguanaces 3, right M3, AG3-2107. Scale bar: 1 mm.

have (part of) their anterior root preserved. This root is also flattened and runs parallel to the posterior one. An I3 from Concu de la Garita (CG-754, MN12) is smaller than the other I3, although this is partly due to dissolution and/or transport. It has a posterior cuspule, and another small cuspule along the lingual crown border. The presence of an anterior-lingual cingulum cannot be confirmed because of the rounding due to erosion. Whereas the posterior root shows the characteristic oblique positioning of I3, the partly preserved anterior root is placed more or less perpendicular to the crown base. In this respect (and in its relatively small size) the specimen differs from other I3 described here. We consider these differences to be too small for separating the tooth taxonomically from the rest of the material. Alternatively, the specimen could represent a DI3.

An upper canine from Los Mansuetos (LM-4005, MN12; Fig. 2(E)) has its main cusp anteriorly placed in a slightly buccal position. Its rounded posterior part is less wide than its anterior part. From the main cusp a blunt, straight crest is running down centrally, where it ends in a small buccally positioned posterior cuspule. A very weak anterior cingulum is present. The two roots are about equally strong, with the straight posterior one being the strongest. The anterior root is slightly curved posteriorly. Because of its relatively small length (Fig. 3), we consider an assignment to *A. aff. depereti* more probable than an assignment to the much larger *P. vireti* or *A. steensmai* nov. sp. (see below). A posterior part of a small-sized upper canine from Prado 15C (PRD15C-186, MN10) is assigned to *A. aff. depereti* as well. Two anterior fragments (ROM3-306 and 307, MN10) also suggest a similar, although somewhat smaller tooth size. Anterior crests are lacking on these specimens. Although the posterior parts of the main cusp area not preserved, onsets of both lingual and buccal cingula are visible.

A small P2 from Prado 3 (PRD3-189, MN10; Fig. 2(G)) has a relatively narrow posterior part, although it is broader than in the specimen of *A. depereti* from Sansan (MN6) as figured by Engesser (1980: fig. 24b), which, unlike the specimen from Prado 3, also lacks a posterior cuspule. On the other hand, P2 from La Grive (MN7/8; Mein and Ginsburg, 2002) have their posterior part well developed, with lingual and buccal sides “égalemodérément bombées” (moderately inflated to a similar degree), a configuration fitting the one in Fig. 2(G). In addition, our specimen contains a well-developed anterior cingulum, a feature also described for the La Grive P2. Except for a slightly narrower posterior part, our specimen is almost identical to an unidentified erinaceine P2 from Cañada 6 (MN9) from the neighboring Calatayud-Montalbán Basin, ~100 km North of Teruel (Lopez-Guerrera et al., 2011: fig. 2(18); note that ‘p2’ should be ‘P2’ in their text). As it cannot be decided with certainty whether this specimen belongs to *A. depereti* or *A. aff. depereti*, we think a designation *A. cf. depereti* for this early late Miocene specimen would be appropriate.

Two P2 were recovered from Los Aguanaces 3 (AG2-2112 and 2113, MN11; Fig. 7(B)). Their posterior part is better developed compared to that of the Prado 3 specimen, with an occlusal outline that is more or less rectangular, except for the anterior edge, which is relatively rounded. The extended postero-lingual corner is lower than the rest of the crown, thereby creating a large, obliquely positioned cutting blade. From the main, pointed cusp a buccally placed, sharp ridge descends towards the postero-buccal cuspule. From this cuspule a cingulum runs downward and anteriorly towards a small lingual cuspule placed halfway the lingual border. Other cingula are present lingually and anteriorly.

Complete Miocene erinaceine tooth rows found in France and Anatolia (*Mioechinus oeningensis*, *M. tobieni*) show that the sub-rectangular outline, as observed for the P2 from AG3 and CG, is caused by the lingual extension of the posterior part of the tooth crown, resulting in an apparently oblique positioning with regard to the overall tooth row direction (e.g., Engesser, 1980: fig. 28).

Because such a lingual extension is less distinctly present in *A. depereti* from Sansan (formerly named ‘*M. sansaniensis*’, see same figure), we assume that it developed during the evolution from this species towards *A. aff. depereti*.

An unworn P3 from Pedregueras 2C (PED2C-1311, MN9; Fig. 7(A)) has the shape of a right-angled triangle, the right angle being the antero-buccal corner. Its buccal part is dominated by a large paracone, from which a sharp ridge is descending towards the posterior apex, from where it is curving back lingually. The lingual part is separated from the buccal part by a groove. It contains a pointed protocone, which is smaller than the paracone. The asymmetric shape of the P3 is more similar to that of *A. depereti* (Engesser, 1980: fig. 24) than to that of *P. intermedius* (Mein and Ginsburg, 2002: Fig. 8; Engesser, 2009: fig. 49), of which the lingual part is poorly developed, rounded and placed more centrally, and *P. vireti*, of which the P3 from its type population Viladecaballs shows a very poorly developed lingual part containing only a low, anteriorly positioned protocone. A second *A. aff. depereti* P3 from Vivero de Pinos resembles PED2C-1311, although its posterior border is less emarginated, and its preprotocrista is continuous. A third, relatively small specimen from Los Aguanaces (AG, MN11) has its posterior margin emarginated and its preprotocrista uninterrupted. Three DP3 from Vivero de Pinos (VIP, MN11) have their lingual parts strongly reduced compared to P3. A sign of a protocone is nevertheless visible on two specimens.

A fragment of a P4 from Masía de la Roma 11 (ROM11-309, MN10) contains the lingual parts of the protocone and hypocone. Because cusps are sharp and curved rather than blunt, we tentatively assign the specimen to *A. aff. depereti* (and not to *P. vireti*). A buccal part of a P4 from Los Aguanaces shows a distinct

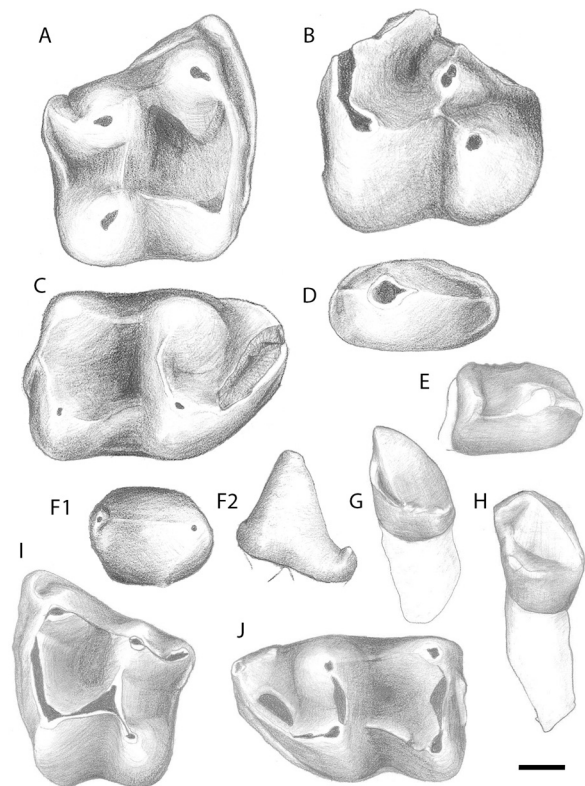


Fig. 8. A–F. *Atelerix steensmai* nov. sp. A: right M2, MDV2-4072, holotype; B: left M1 (fragm.), MDV2-4064; C: right m2, MDV2-4074; D: left C, MDV2-4067; E: right i3, MDV2-2054; F: right P2, MDV2-4068 in occlusal (F1) and buccal (F2) views. **G, H.** Erinaceinae genus and species indet. from Los Aguanaces 3. G: left I2, AG3-2102; H: left I3, AG3-2103. **I, J.** *Atelerix* aff. *depereti* from Concu de la Garita and Los Mansuetos. I: left M2, LM-2002; J: left m2, CG-752. Scale bar: 1 mm.

posterior emargination, which points to a low degree of molarization. Also this feature would exclude an inclusion into *Postpalerinaceus vireti*, the P4 of which hardly show a posterior emargination, and whose anterior and posterior borders tend to run parallel (Crusafont and De Villalta, 1947; see also López-Guerrero et al., 2011).

Three M1 of MN11 age (AG, VIP, PM) have a sub-squared shape without a strong metastyle (as for example in *P. intermedius*). The W/L ratios of 1.13 and 1.04 for the specimens from AG and VIP (the end part of the metastyle is broken off in the PM specimen, Alcalá et al., 1991: pl. 1, fig. 38) are low compared to ratios of rectangular shapes, such as in '*Amphechinus*' *robinsoni* from Manchones (1.35), being somewhat more close to ratios of squared shapes, like in *P. vireti* from Viladecaballs (1.00; Crusafont and De Villalta, 1947) and Can Llobateres (1.00–1.03; Crusafont and Gibert, 1974). Borders are relatively straight, a condition that is also different from that in *P. vireti*, in which emarginations characterize all sides (as in P4), including the anterior one (see especially the drawings in Crusafont and Gibert, 1974.) All four main cusps in M1 are well developed. The protocone is the strongest cusp. A distinct metaconule is present, whereas a protoconule is only faintly visible. An anterior cingulum is present, which broadens in buccal direction. The strength of the posterior cingulum is variable. The vestige of a lingual cingulum is present between the protocone and hypocone in the VIP and AG specimens.

An M2 from Los Mansuetos (LM-4002, MN12; Fig. 8(I)) has four well-developed main cusps. The position of the hypocone is slightly posterior to that of the metacone. Strong ridges connect the protocone with the paracone on the one hand, and with the metacone and hypocone via the metaconule (present as a swelling) on the other hand. The paracone and metacone are connected by a low crest. The protoconule is lacking. A buccally widening cingulum is present along the anterior border, and a second cingulum is present posteriorly. Whereas a buccal cingulum is lacking in LM-4002, another, fragmented specimen from the same site (LM-4001) shows a short cingulum-like structure in the middle of the buccal border. LM-4002 resembles the much older M2 of *A. depereti* from Sansan (MN6, Engesser, 2009), except for a much larger size and some details of the morphology, such as a complete instead of interrupted connection of the protoloph with the paracone. Similarities are even larger to the M2 from Petersburg 6 (MN7–8, Germany) classified as '*Mioechinus*' sp., both in terms of size and morphology (Ziegler, 2005: fig. 4K).

Although M2 size is similar to that of *P. vireti*, the occlusal morphology of the latter species is different, with the metaloph and metaconule placed in a more posterior position (both in Viladecaballs and Can Llobateres, MN9; Crusafont and De Villalta, 1947; Crusafont and Gibert, 1974). In addition, the W/L ratio is lower in *P. vireti* (1.09 and 1.02) than in the Los Mansuetos specimen (1.18), which, in turn, are similar to average values for *A. depereti* from the various fissures of La Grive (MN7 fissures: 1.16 and 1.21, MN8 fissures: 1.13 and 1.19), but smaller than the value for *A. depereti* from the MN6 locality Sansan (1.24). A still larger value of 1.29 characterizes the M2 of '*Amphechinus*' *robinsoni* from the MN6 site Manchones (Gibert, 1975; Fig. 4).

M2 from Los Aguanaces and Vivero de Pinos (MN11) resemble the Los Mansuetos specimen in size and shape. W/L ratios are somewhat smaller (1.15 and 1.10, respectively). Whereas a metaconule can be observed to be present on the AG specimen, it is hardly visible on the specimen from VIP. Also, the morphology of a buccal fragment of an M2 from Pedregueras 2C (PED2C-1314, MN9) fits that of LM-4002 (Fig. 8(I)), showing a metaconule and a posterior emargination that is not acute. Unlike this specimen, PED2C-1314 has its protoloph interrupted close to the paracone, and a very thin buccal cingulum. Because no features were observed that contradict an assignment to *A. aff. depereti*, two small

fragments of M2 from Masía de la Roma 3 and Prado 15C were tentatively assigned to this species as well.

Two unworn M3 from Masía de la Roma 3 (ROM3-301, MN9) and Masía de la Roma 7 (ROM7-260, MN10; Fig. 7(D)) are very similar in size and shape. Their outline is elongated and more or less ellipsoid. The ROM7 tooth is slightly more robust and its cusps are somewhat better developed. Three cusps are present, the height of which decreases in buccal direction. The lingual and intermediate cusp (protocone and paracone according to Butler, 1948: fig. 13) are integrated into a main ridge. The more isolated, buccal cusp (parastyle) is connected to the intermediate cusp via a small ridge. No roots are preserved. A slightly larger, unworn M3 from Tortajada A (TOA-2001, MN11) is similarly shaped, although its cusps are more individualized, as evidenced by the presence of a valley behind the ridge between the almost equally important protocone and paracone. The main ridge, which integrates both main cusps, is slightly curved anteriorly, in contrast to the straighter shape in the Masía de la Roma specimens. A tiny, short crest is running down posteriorly from the lingual cusp. The parastyle is low, as in the ROM specimens, but it is more isolated, being connected to the paracone by a very tiny ridge only. A small and short cingulum-like ridge is present postero-lingually. No root(s) are preserved. Two specimens from Vivero de Pinos (VIP, MN11) have a similar size, outline and simple cusp pattern as the specimen from Tortajada A. Like M2, also the M3 are similar in size and shape to M3 of the form classified as '*Mioechinus*' sp. from Petersburg (Ziegler, 2005: fig. 4L).

A small i3 from Masía del Barbo 2A (MBA-2084, MN10) is very low-crowned, resembling the i3 of *A. depereti* from La Grive (Mein and Ginsburg, 2002). Its buccal border is relatively straight, whereas the lingual border is strongly convex. Its antero-buccally placed main cusp is elongated longitudinally, constituting a narrow antero-posteriorly running ridge. Posteriorly, this ridge ends in a small cuspule, from where a cingulum is running along the postero-lingual part of the tooth. Another i3 from the similarly aged site Masía de la Roma 9 (ROM9-158, MN10), which lacks its lingual face, fits the MBA specimen well in size and morphology. Four other i3 from Masía de la Roma 9, Los Aguanaces 3 and Conclud 3 (AG3-2110, MN11; CC3 3016–3018, MN12) have a similar shape, except for a more developed postero-lingual corner and stronger posterior cingulum, which looks like a true ridge. The relatively large specimen from Los Aguanaces 3, which is postero-buccally damaged, has its posterior ridge positioned somewhat more buccally than the MB2A specimen. A similarly aged specimen from VIP has its posterior ridge placed relatively buccally as well.

Two lower canines from Prado 15C (PRD15C-185,187; MN10) are asymmetrical bucco-lingually, because of the buccally placed central ridge. The main cusp is positioned anteriorly. The large lingual face is slightly concave. The central ridge, which descends from the main cusp, ends in a small posterior cuspule that resides on a cingulum. The single root (PRD15C-187) is flattened antero-posteriorly. Another specimen from Masía de la Roma 3 (ROM3-302, MN9) has a damaged occlusal surface, preventing close inspection of the central ridge and posterior cuspule. It is relatively short, showing a cingulum anteriorly and postero-lingually. Its root is flattened anteriorly. A lingual fragment with a partial root from Cascante 7A (CASC7A-9, MN10) fits the ROM3 specimen in terms of morphology and is attributed to *A. aff. depereti* as well.

An unworn p3 from Masía del Barbo 2A (MBA-2083, MN10; Fig. 7(C)) has a triangular shape with its buccal and lingual sides converging towards the anterior apex. Its moderately strong central cusp is pointed. From this cusp a sharp crest is running towards the anterior apex, where a cuspule is formed. Strong lingual and posterior cingula enclose a concave valley. The posterior cingulum is strongest lingually, where it tends to form a cuspule. Four other p3 (MBB-2052, CG-755-756, CC3-3020) have

a similar triangular shape, but their width-length ratio is lower. Also these specimens are characterized by a pointed main cusp and a pointed anterior apex, which is bended up and carrying a small cuspule. The posterior cingulum supports a centrally placed posterior cuspule. MBB-2052 (MN10) shows little cingulum development, but possesses a distinct posterior cuspule and a smaller anterior cuspule. CG-755 (MN12; Fig. 2(F)) resembles MBA-2083, although it is smaller and more elongated with less well developed cingula. The single and strong posterior root (as preserved in both CG specimens) is directed posteriorly, but less obliquely than in *i3*. It is antero-posteriorly flattened. The specimen from Concud 3 (MN12) is somewhat rolled off, but still shows posterior and anterior cuspules. Its strong, obliquely placed root is square-shaped.

The combination of an anteriorly pointed shape and broad posterior part is characteristic for the *p3* of *A. depereti* (Mein and Ginsburg, 2002). By contrast, *p3* of *P. intermedius* (Mein and Ginsburg, 2002: fig.17, re-identified herein as a left specimen) are somewhat more inflated as especially expressed by a more rounded antero-buccal border.

The *p4* is represented by two fragments only. A buccal fragment from Puente Minero 2 (PM2-202, MN10) shows the remains of a metalophid that is running backwards. A fragment from Prado 3 (PRD3-188, MN10) could only tentatively be assigned to *A. aff. depereti* based on the attribution to this species of another element (*P2*).

The lower first molar is poorly represented as well. An isolated talonid from an *m1* from Vivero de Pinos suggests an original width of ~2.7–2.8 mm, much smaller than the width of *m1* of *Postpalerinaceus vireti* (Fig. 6). It is assigned to *A. aff. depereti*, the smaller-sized form found at this site. An antero-lingual fragment (AG3-2111, MN11), which only contains paraconid and metaconid, is also assigned to this species.

An *m2* from Concud Cerro de la Garita (CG-752, MN12; Fig. 8(J)) has its talonid and trigonid sub-equal in length. Its lingual side is slightly convex at the position of the metaconid. A thin and short ridge runs posteriorly of the cusp-shaped paraconid and partly closes the trigonid. The posterolophid is not free ending, but meets with the upward running posterior cingulum at the base of entoconid. The posterior cingulum ends at the base of the hypoconid, but resumes as a buccal cingulum running all the way to the anterior apex. A similarly-sized specimen from Vivero de Pinos (MN11) has its paraconid more ridge-shaped than the specimen from Concud Cerro de la Garita.

Two minimally worn *m3* from Prado 15C (PRD15C-3, MN10) and an unworn *m3* from Concud Cerro de la Garita (CG-753, MN12; Fig. 2(H)) are very similar in size and shape. They basically consist of a trigonid only. The protoconid is slightly stronger than the metaconid. The paraconid is incorporated into a ridge that connects it with the metaconid and which rounds the anterior apex. The trigonid is open buccally. A younger specimen from La Gloria 5 (MN13) is similar in size and shape, whereas two specimens from Vivero de Pinos (MN11) are somewhat larger. One of these has its anterior ridge extending relatively far backward along the lingual side, without closing the trigonid.

Atelerix steensmai nov. sp.

Figs. 8(A–F)

2001. Erinaceinae indet. – Van Dam et al.

Derivation of name: in honor of Dr. Karel Steensma, for his significant contribution to mammal paleontology and stratigraphy, including various fieldwork campaigns in the Teruel Basin and other Spanish basins.

Holotype: RM2, no. MDV2-4074, stored in the Department of Earth Sciences, Utrecht University, the Netherlands (Fig. 8(A)). L = 4.59 mm, W = 5.27 mm.

Paratypes: 1 LI2, 1 RC, 1 RP2, 2 RM1, 1 RM2, 2 Ri3, 1 Lc, 1 Lp4, 1 Lm1, 2 Lm2, 1 Rm2.

Type locality and biostratigraphy: Masada del Valle 2 (MDV2), Teruel Basin, east Central Spain. Local Biozone: L; Mammal Neogene Unit: MN12; Age: 7.6 Ma. (Van de Weerd, 1976; Van Dam et al., 2001).

Occurrence: besides type locality: Masada Ruea (MRU3; Fig. 1): 1 LP2, 1 Lp4, 1 Rm2.

Measurements: see Table 3.

Diagnosis: Large erinaceine, with size comparable to that of *P. vireti*. Strong development of cusps on upper and lower molars; development of ridges subdued. Outline of M1–2 squared; buccal and posterior emarginations very shallow. Upper incisors (I2) pointed and relatively symmetric; upper canine with anterior crest. P2 rounded and with two roots. M1–2 without protoconule, but M1 with strong metaconule. M2 without metaconule and without centrally placed crests (metaloph and hypocone crest), but with direct connections of the hypocone with both protocone and metacone, resulting in a squared pattern of connections between the four main cusps. *i3* low-crowned, wide posteriorly and with buccally placed central crest. Bulbous lower canine. *m1* with paraconid and especially metaconid positioned relatively buccally. *m2* with squared talonid with shallow buccal emargination, and with very poorly developed ridges between metaconid and entoconid and between protoconid and hypoconid. Lingual ridge posteriorly of paraconid of *m2* short, thereby creating an open trigonid.

Differential diagnosis: Differs from *Atelerix* (aff.) *depereti*, *Mioechinus tobieni*, *Postpalerinaceus intermedius* and *P. cingulatus* by its larger size, and by its molar morphology, which is characterized by straighter borders and a stronger development of cusps at the cost of ridges. Differs from *P. vireti* in its flattened and more symmetric I2, its development of straight borders and squared pattern of the main ridges and the absence of a metaconule in M2, the flat occlusal surface of *i3*, its less bulbous lower canine with central cusp positioned more anteriorly, and its *m2* with straightened buccal border, well-developed cusps and poorly developed longitudinal ridges.

Description and comparison:

Type material. Although much larger, the I2 from Masada del Valle 2 (MDV2-4051, MN12) has a crown morphology that is superficially similar to that of *A. aff. depereti* from ROM7 (MN10; described above), which contains a similarly shaped, relatively narrow, lingually positioned climbing main ridge. The main cusp is slightly less pointed than in the ROM7 specimen, because of a less concave postero-lingual face, yielding a more symmetric shape in postero-lingual view. MDV2-4051 shows a short continuation of the cingulum beyond the meeting point with the posterior central ridge, where a small cuspule is present. No root is preserved.

The crown of the upper canine (MDV2-4067; Fig. 8(D)) is dominated by one strong main cusp and a longitudinal crest that extends across the entire length of the tooth. The anterior part of this crest is shifted lingually. The lingual face of the tooth is slightly concave. A narrow antero-lingual cingulum is present. The posterior cingulum stands out as a small plateau. Lingually, it reaches a point half-way the tooth, at the level of the main cusp tip. Two strong roots are present, with the posterior one being the strongest. It has its posterior side rounded.

The P2 (MDV2-4068; Fig. 8(F1,2)) has its central crest shifted buccally. This crest ends in a cuspule posteriorly. No other posterior cuspules are present. Posterior and anterior borders are rounded, resulting in a symmetric shape in occlusal view. A poorly developed antero-lingual cingulum is present. The P2 has two antero-posteriorly flattened roots.

Two lingual parts of M1 (MDV2-4074, 4075; Fig. 8(B)) show a very strong metaconule, situated buccally of the meeting point of

hypocone crest (entoloph) and postprotocrista. Lingual borders are relatively straight, a condition opposite to that in *Postpalerinaceus*, in which the M1 shows a strong re-entrant between protocone and hypocone. MDV2-4075 contains a little cingulum-like ridge between proto- and hypocone.

The complete M2 (MDV2-4072; Fig. 8(A), holotype) is relatively squared due to its large length. All four main cusps are well developed and there is no sign of a meta- or protoconule. The connection between protocone and hypocone is straight and not curving inward to form a postprotocrista, the result being a squared pattern of connections between the four main cusps. Except for a strong protoloph, ridges are poorly developed. Cingula are absent both lingually and buccally of the metacone. The anterior cingulum is strong and widening buccally.

The shape of three i3 (MDV2-4053, 4054, 4055; Fig. 8(E)) is similar to that of *A. aff. depereti*, although the teeth are much larger and relatively wide posteriorly, with a central ridge that is placed more buccally. The remnants of a single, posterior root show that it was pointing in posterior direction.

The bulbous lower canine is similarly-shaped as in *A. aff. depereti*, except that it is less asymmetrical bucco-lingually. It is similarly-sized as the lower canine on the holotype of *Postpalerinaceus vireti* from Viladecaballs, but the latter specimen is even more bulbous, with a central cusp that seems to be positioned less far anteriorly.

The buccal half of a p4 shows a high protoconid, which descends towards a narrow posterior valley, behind which the buccal part of a tiny posterior ridge can be discerned.

The isolated trigonid from an m1 (MDV2-4071) has its paraconid and especially its metaconid positioned relatively buccally. This configuration is unlike that in *P. vireti*.

A complete m2 (MDV2-4061; Fig. 8(C)) has cusps that are relatively isolated with large trigonid and talonid basins in between. Metaconid and entoconid are stronger than protoconid and hypoconid. The anterior apex is rounded with the paraconid shaped as a ridge. Ridges between metaconid and entoconid and between protoconid and hypoconid are virtually absent. The lingual ridge posteriorly of the paraconid is short, which results in an open trigonid. The short posterior cingulum runs downward, until it abruptly ends. Its upper end is connected to a thin posterolophid. A weak buccal cingulum extends along the trigonid part of the tooth. Also, an isolated talonid (MDV2-4076) shows a very weakly developed posterolophid that almost disappears in the middle of the posterior border.

Other material. Masada Ruea 3 (MN12), which is geographically very close to Masada del Valle 2 (Fig. 1), has a very similar age (Van Dam et al., 2001). A P2 from this site (MRU3-364) is equal in size and shape to MDV2-4068, with a sub-rectangular outline with rounded corners, an anteriorly placed, sharp main cusp, and a buccally placed central ridge.

A fragment of a p4 (MRU3-363) shows a curved metalophid that descends posteriorly along the lingual border towards a small entoconid without forming a metaconid and leaving the trigonid wide open lingually. The posterolophid carries an elongated cusp in the middle and runs down towards the postero-buccal corner, which is low compared to the postero-lingual corner.

An m2 (MRU3-231) resembles MDV2-4061 in its straight buccal border, in a small ridge posteriorly of the paraconid (leaving the trigonid partly open), and a posterior cingulum that extends downward to grade into a very thin basal cingulum, which continues until the anterior apex (with an interruption at the level of the hypoconid).

Remarks: The strong development of cusps at the expense of ridges on the molars as observed in *A. steensmai* nov. sp. has not been observed so far in other Miocene lineages. On the other hand, the morphology of various anterior elements (for instance, the

flattened I2 and i3, and the shape of the lower canine) echoes features observed in *A. aff. depereti*, suggesting a phylogenetic relationship. Because ridges are also relatively subdued in species of modern *Atelerix* (e.g., *A. albiventris* vs. *Erinaceus intermedius*; Gould, 2001), we prefer the assignment to this existing genus instead of erecting a new genus.

Erinaceinae indet.

Figs. 7(G), 8(G, H)

Measurements: see Table 4.

Description: Three teeth from Los Aguanaces 3 (an I2, I3 and M3) could not be assigned to any of the other species. The I2 and I3 clearly belong to the same species, as both specimens show the same particularly style of fossilization, with a beige crown and dark brown root. The M3 perhaps belongs to the same species as well, but could also represent another form.

The intermediately-sized I2 from (AG3-2102, MN11; Fig. 8(G)) shows a rounded circumference of both the crown and the root (excluding an assignment to the *Atelerix* species described above), and has a very robust and protruding lingually and upward running cingulum ridge that extends all the way up towards the anterior part of the crown (excluding assignment to *Postpalerinaceus vireti*).

The morphology of the I3 (AG3-2103; Fig. 8(H)) is very different from that of the other I3 described in this study. Its shape is compact instead of elongated (e.g., as in Engesser, 1980: figs. 22, 23). The tooth is characterized by a flattened, triangular-shaped “carnassial” blade with both anterior and posterior ridge well developed. The posterior cingulum is elevated to form a plateau-like postero-lingual rim. This rim is not reaching as far anteriorly as its homologue in the I2. The I3 contains only one very strong root, which is directed vertically. The presence of one root in I3 is not very common in erinaceines; for instance, it has been observed in populations of modern *A. albiventris* (Gould, 2001), thereby creating a tension with the genus diagnosis (Frost et al., 1991).

The M3 from the same site (AG3-2107, MN11; Fig. 7(G)) has a sub-triangular to drop-like shape. Its intermediate cusp (paracone) is only slightly smaller than its lingual cusp (protocone), to which it is connected by a curved crest. The buccal cuspsule (parastyle) is relatively isolated from the paracone (more than in *Atelerix aff. depereti*; Fig. 7(D)) and is connected to it by a very thin ridge only. The AG3 specimen has well-developed cingula along both long sides. It contains a large, broad root, because of the fusion of its lingual and buccal part. The type of outline, the presence of a parastyle, and the well-developed cingula, are features that are also observed in *A. depereti* (Mein and Ginsburg, 2002; Engesser, 2009). Differences include a smaller size and the presence of two (partly fused) roots in *A. depereti*. The shape of the tooth is very similar to that of the recent *Atelerix albiventris* (Gould, 2001). Another observed feature described for *Atelerix* is the presence of a small ridge behind the protocone, which may be homologous with the hypocone (Butler, 1948).

Besides the AG3 material, three Erinaceinae fragments from Masía de La Roma 4B, Prado 3, and Patrimonio Forestal 5A (ROM4B-73, PRD3-190, PF5A-52) could not reliably be assigned to a specific element, let alone to one of the species (Fig. 9).

5. Discussion

5.1. Iberian distribution of Neogene erinaceines

We have identified four different species of Erinaceinae in the upper Miocene (MN9-MN13) of the Teruel and Calatayud-Montalbán Basins. Large-sized erinaceines are represented by *Postpalerinaceus cf. vireti* and *Atelerix steensmai* nov. sp. Middle-

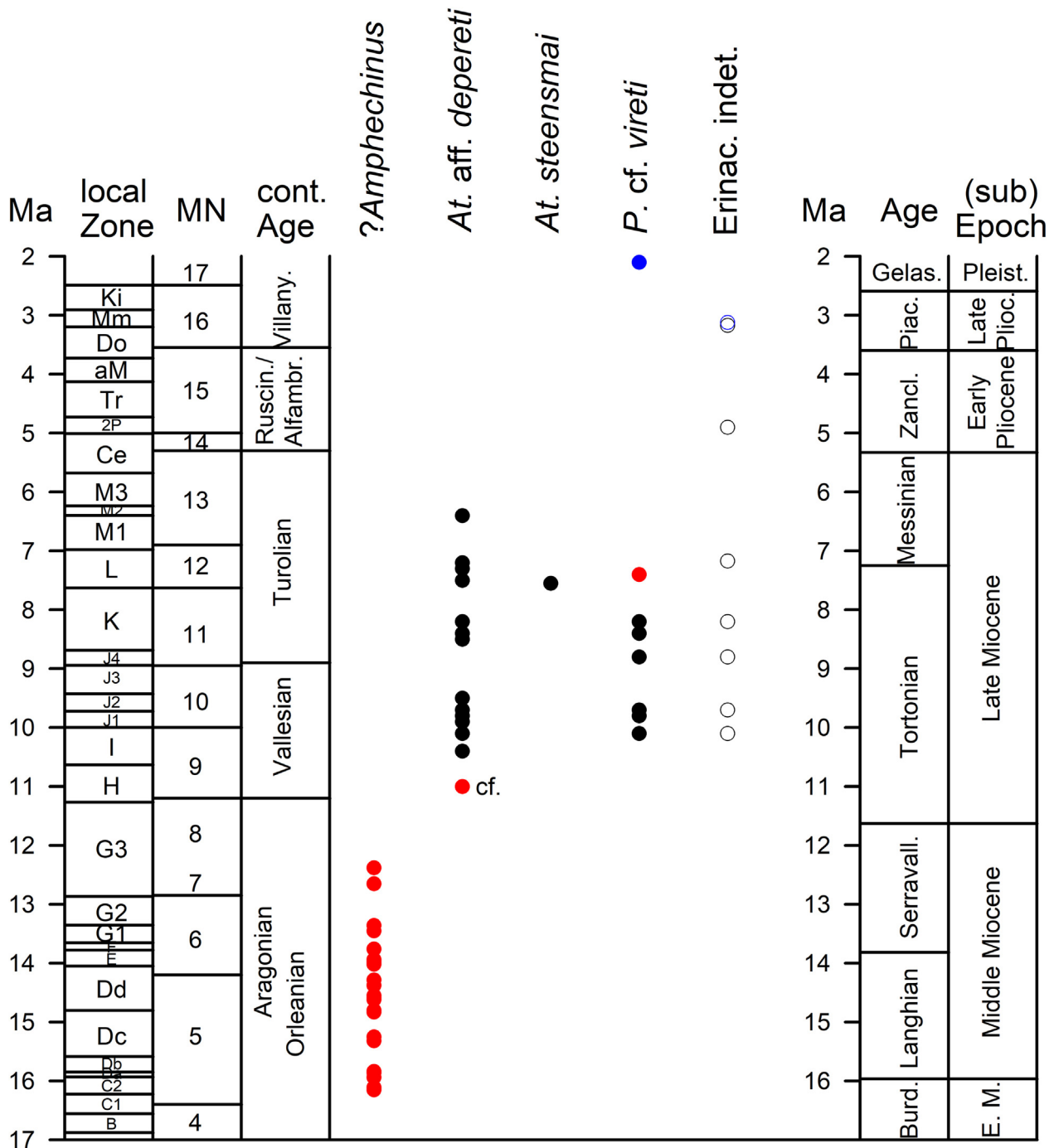


Fig. 9. Temporal distribution of Erinaceinae between 17 and 2 Ma in the Teruel Basin (black; this paper), Sarrión depression (blue; Adrover, 1974; Crochet and Heintz, 1971), and Calatayud-Montalbán Basins (red; López-Guerrero et al., 2011; Van der Meulen et al., 2012; with approximate ages for Cañada 6 (11.0 Ma) and 12 (7.2 Ma) based on López-Guerrero et al. (2011) and van Dam et al. (2014). Ages local Zones after Van Dam et al. (2006, 2014, ongoing work). Ages MN and marine units after Hilgen et al. (2012) (For interpretation of the references to colour in this figure legend, the reader is referred to the web version of this article).

sized forms are represented by *Aterlix aff. depereti*, the most common erinaceine, and by a very rare, indeterminate form from Los Aguanaces 3, the genus and species identifications of which have been left open (Erinaceinae indet.). Alpha diversity is maximal in the middle part of the study interval (MN11), with three species recorded in the single locality Los Aguanaces 3.

A small temporal gap in spiny hedgehog occurrence is recorded within MN10 (corresponding to the upper part of Zone J2 and Zone J3). More remarkably, however, is the virtual absence of spiny hedgehogs after MN12, with only a single occurrence in MN13 (La

Gloria 5; Mein et al., 1990). Also, the Pliocene record of the Teruel basin is very poor in Erinaceinae (Mein et al., 1990), with one occurrence in MN14 (La Gloria 4) and one in MN16 (Escorihuela). Two other younger occurrences have been reported for the neighboring Sarrión Depression, one from MN16 (Sarrión 1; Adrover, 1974), and one from MN17 (La Puebla de Valverde, MN17; Crochet and Heintz, 1971). The material from the latter site (a partial mandible with m2 and partial m1, and a p4) was classified as *Postpalerinaceus cf. vireti*, although according to the authors it could also represent a separate species.

The best represented species in our material, *Aterlix* aff. *depereti*, covers the entire study interval. We consider this form to be a direct descendent of *A. depereti*, a smaller-sized form known from the late middle Miocene of France. Although *Aterlix* aff. *depereti* is larger than *A. depereti* across most of its range, size reduction seems to have taken place towards the end of its record (Concud Cerro de la Garita, MN12), with dimensions of at least the anterior elements approaching that of *A. depereti*. *Aterlix steensmai* nov. sp. is restricted to the older part of MN12, and is considered to be the result of a separate development towards larger size and stronger bunodonty within the *Aterlix* genus. The presence of *Postpalerinaceus* (cf.) *vireti* in the Teruel Basin is not surprising given the temporal overlap with the record of this species in NE Spain (Vallès-Penedès Basin, MN9–10). With our new finds, the late Miocene temporal occurrence of this species has been further extended to MN11. Afterwards (MN12), it seems to have been replaced by the similarly-sized *A. steensmai* nov. sp. in the Teruel Basin. Interestingly, a large P4 identified as cf. *Postpalerinaceus* was found in the MN12 site Cañada 12 in the neighboring Calatayud-Montalbán Basin (López-Guerrera et al., 2011). Its outline hardly shows a posterior emargination, and contains anterior and posterior borders that almost run parallel, features that also characterize the morphology of the P4 on the holotype of *Postpalerinaceus vireti* from Viladecaballs (MN9, Vallès-Penedès Basin). We therefore believe that its generic assignment could be narrowed down to *P. cf. vireti*.

Because a revision of the Vallès-Penedès Basin erinaceines is not intended here, we confine ourselves to a few observations on the material from this basin. Firstly, from the viewpoint of both size and morphology, the exclusive presence of *Postpalerinaceus vireti* in the interval corresponding to later MN9 and MN10 may be considered doubtful. For instance, various specimens from Can Ponsic (~10.1 Ma), a locality supposed to contain *Postpalerinaceus vireti* (Crusafont and Gibert, 1974), are consistently smaller than those from Can Llobateres (9.7 Ma) and Viladecaballs (~9.4 Ma). Such smaller-sized specimens also occur in the collection of the *P. vireti* type locality Viladecaballs itself. Generally, these smaller-sized teeth tend to have a less derived habitus. Furthermore, several differences between *P. vireti* material from Viladecaballs and Can Llobateres are difficult to reconcile with the presence of only one species. These differences are most evident for P3 (Fig. 4): P3 length is exceeding width in Viladecaballs ($L = 2.15$ mm, $W = 1.60$ mm, $W/L = 1.19$; Crusafont and De Villalta, 1947), whereas the situation is reversed in the P3 from Can Llobateres, for which the W/L ratio is only 0.85 (Crusafont and Gibert, 1974). Furthermore, the figured M1 from Can Llobateres in the latter study shows an extreme morphology with emarginations at all sides (as in P4), a configuration that is difficult to match with that of the type specimens from Viladecaballs. Unfortunately, the type material is heavily worn, hampering any detailed comparisons with regard to occlusal features. In our opinion, the holotype cranial material of *Postpalerinaceus* material needs to be re-studied (involving some additional preparation) in order to substantiate presumptions (e.g., Ziegler, 2005) that the lacrimal foramen is situated outside the orbit (invalidating potential synonymy of *Postpalerinaceus* with *Amphechinus* and assignment of the species *intermedius* to *Postpalerinaceus*) and that the basisphenoid groove is absent (invalidating potential synonymy of *Postpalerinaceus* with *Mioechinus*).

In a broader Neogene perspective, the following transitions in Erinaceinae history can be identified for the Iberian Peninsula:

- ~16 Ma: entry of Erinaceinae around the early-middle Miocene transition with the presence of *?Amphechinus* in the Calatayud-Montalbán Basin (Gibert, 1975; Van der Meulen et al., 2012) and Valencia region (Buñol; Robles et al., 1991), and *Mioechinus butleri* in the Vallès-Penedès Basin (Crusafont et al., 1955). An older entry of the group cannot be excluded given that, unlike rodents (e.g., Daams et al., 1996), the late Oligocene to earliest Miocene (~MN1–2) insectivorans from Spanish sites have hardly been studied. Insectivorans from the younger part of the early Miocene (~MN3–4) are nevertheless well-documented (Van den Hoek Ostende, 2003; Van den Hoek Ostende and Furió, 2005; Van der Meulen et al., 2012), and no erinaceines were found. Later, during the later middle Miocene, *Postpalerinaceus intermedius*, a form well-known from France, is known to have entered the Madrid Basin (Paracuellos 5, 13.8–13.7 Ma; Peláez-Campomanes et al., 2003). *?Amphechinus* survives on the Iberian Peninsula at least until the middle-late Miocene transition (Vallès-Penedès Basin; Gibert, 1975), with rarefaction taking place towards the end of the middle Miocene (Zone G; Van der Meulen et al., 2012);
- ~11–10 Ma: replacement of *?Amphechinus* by other species, such as *Aterlix* aff. *depereti* in the eastern Spanish interior as evidenced in the records from the Teruel Basin (this paper) and Calatayud-Montalbán Basin (Cañada 6; López-Guerrera et al., 2011), and by *Postpalerinaceus vireti* in the Teruel basin (this paper), the Vallès-Penedès Basin (Crusafont and De Villalta, 1947; Crusafont and Gibert, 1974) and the Madrid Basin (Cerro de Batallones; Álvarez-Sierra et al., 2017). Except perhaps for the latter occurrence, Erinaceinae have not been recorded so far for the interval ~9.5–9.0 Ma (upper J2 and J3 Zones);
- ~8.5 Ma: temporary increase in species richness (Teruel Basin), culminating in the presence of 4 species between 8.5 and 7 Ma (two species of *Aterlix*, one *Postpalerinaceus*, and one unidentified form);
- ~7 Ma: almost complete local (Teruel Basin) and probably regional (Iberian Peninsula) extinction of Erinaceinae around the Tortonian-Messinian transition. The few reported Pliocene occurrences (La Gloria 4, Teruel Basin, MN14; Gorafe 1 and Baza, Guadix-Baza Basin, MN14; Layna, Soria region, MN15; Escorihuela, Teruel Basin, MN16; Sarrión 1, Sarrión depression, MN16) refer to rare and still undescribed material which is either indicated as Erinaceidae indet. or *Erinaceus* sp. (Adrover, 1974; Mein et al., 1990; Van den Hoek Ostende and Furió, 2005; Furió et al., 2015, 2018; Piñero et al., 2017), although the latter genus assignment should be regarded as uncertain. The youngest known record of pre-modern (i.e., 'non-*Erinaceus*') erinaceines is an occurrence of *Postpalerinaceus* (*P. cf. vireti*), as described for La Puebla de Valverde (MN17, Sarrión depression);
- ~1.5 Ma: entry of undisputed *Erinaceus* in the Lower Pleistocene (with various records across Spain; Furió et al., 2015, 2018).

Before we try to explain this spatiotemporal pattern in the Iberian distribution of spiny hedgehogs, we discuss the dental functional morphology of the group, because it provides a useful source of information on preferred diets and environments of the different lineages.

5.2. Dental variation and diet

Dental morphology reflects dental function, which in the case of mammals includes a broad range of actions such as cutting, crunching, piercing, etc. of both animal and plant food. Although modern spiny hedgehogs basically consume small invertebrates, they are known to supplement or even replace these by other materials such as small vertebrates, eggs, and plant tissue (Corbet, 1988; Reeve, 1994). The dentitions of the more advanced fossil forms described here are expected to reflect this multi-purpose aspect. In an attempt to functionally and ecologically interpret the erinaceine dentition, we relied on works such as that of Lucas (2004), who focuses on tooth shape in relation to the physical

properties of the different food types, and on the various studies of Freeman on modern bats (Freeman, 1979, 1984, 1992, 1998). Part of this latter group has a dental morphology that is comparable to that of erinaceines, although dietary specializations in bats have proceeded further, covering almost all major dietary types (including carnivory, frugivory, 'nectarivory', etc.; Freeman, 1998), and the dentition might also be affected by cranial constraints associated with their aerial locomotion.

Of the genera discussed in this work, *Amphechinus* has the oldest and most primitive dental pattern. The dentition of this genus (especially in the oldest forms) still resembles the classical tribosphenic design. The presence of many small sharp ridges all across the entire dentition points to the ability to surmount the 'fracture toughness' of insect cuticles, which are stiff composites with fiber layers in different directions, thereby resisting crack propagation (Lucas, 2004). It can therefore be assumed that these forms mostly consumed small invertebrates, which they could manipulate using their relatively large incisors (a typical feature in Erinaceinae; Butler, 2010), pierce and immobilize with their knife-like canines, and chop into small pieces using their molars and premolars. In this respect, the typical W-shaped ectolophs that characterize insectivorous upper dentitions in Insectivora and Chiroptera may be viewed as arrays of 'mini-carnassials' that break up small invertebrates, while at the same time holding the fragments in place (Freeman, 1979). The smaller size of especially the oldest representatives would, however, set a limit to prey size (see also Pfretschner, 1997). *Atelerix* (aff.) *depereti*, the dentition of which contains sharp blades (e.g., I3, C, and P2; Figs. 2(D, E), 7(B); Engesser, 2009: fig. 48), and many sharp, small-sized ridges, would still largely have conformed to such an 'invertivorous' diet. However, the beginning molarization (relatively squared molars) suggests a somewhat less 'invertivorous' diet than for *Amphechinus*, implying a more 'mainstream' hedgehog (varied) menu consistent with the diet of living *Atelerix* (Reeve, 1994; Santana et al., 2010).

More advanced *Postpalerinaceus* such as *P. vireti* show a reduction of the P3, molarization of the fourth premolars, and a development towards square-shaped M1-2 containing additional cusps (meta- and protoconule). *Postpalerinaceus* shares these features with modern *Erinaceus* and *Atelerix*, which also have these two conules present (although in modern *Atelerix* the protoconule may be missing; Gould, 2001). Anterior elements in *Postpalerinaceus* are stout, rounded, and well secured. The presence of large and robust teeth allows for durophagous action, i.e., the crunching and fracturing of hard items such as beetle carapaces, snails and scales of small reptiles. The remarkable horizontally flattened wear surface on the lower canine (Fig. 2(C1,2)) and premolars as encountered in La Gloria 10 could suggest a predisposition for crushing or resisting such hard objects (bone, reptile shale?). Perhaps *P. vireti* also scavenged nests or similar places where young grow up (Álvarez-Sierra et al., 2017). In addition, analogous to carnivores, the possession of a strong carnassial pair, as observed in *Postpalerinaceus* (large P4 blade and elongated trigonid of m1), would allow for efficient cutting across 'soft solids' such as skin or muscle of small vertebrates. Nonetheless, there will have been limits to such shearing action because of size. As observed in the slightly smaller-sized modern *Erinaceus*, persistent biting rather than carnassial shearing may have been used for killing vertebrate prey (Reeve, 1994).

Molarization (with an increase of cusp area at the expense of crest area) would also have facilitated the crushing and grinding of plant tissue. The advantage of a full functioning hypocone that sinks into the trigonid, duplicating the action of the protocone in the talonid, is obvious (Pfretschner, 1997). In our material, molarization and cusp development is particularly well developed in *A. steensmai* nov. sp., where the absence of structures in the

middle part of the M2 creates a basin that functions as a 'mortar', the 'pestles' being the cusp-shaped entoconid and hypoconid of the m2 (Butler, 1948). The relatively straight lingual border of the M2 further contributes to a widening of its central basin.

Canines typically constitute the loci of the first action in fracturing and immobilizing prey. *Postpalerinaceus vireti* has rounded upper canines without an anterior longitudinal crest and only a weak posterior crest (observation on holotype). By contrast, the upper C of *A. steensmai* nov. sp. shows distinct anterior and posterior crests. Also, the posterior fragment of a C of *Atelerix* aff. *depereti* from Prado 15C shows at least the presence a clear centrally positioned, posterior crest. In carnivores, strong and rounded canines are thought to prevent breakage by prey bones (Van Valkenburgh and Ruff, 1987; Freeman, 1992). In bats, edges on upper canines are thought to have a function in directing cracks both towards incisors (including clipping off inedible parts) and (pre)molars (further cutting by ectolophs), with movement confined by occlusion of upper and lower canines (Freeman, 1992). Following this argument, species such as *A. steensmai* nov. sp. would be better predisposed to durophagy (with the need for making cracks) than to carnivory, whereas *Postpalerinaceus* would be well equipped for both types.

Land snails, a very common group of fossils in the Teruel basin (Albesa and Robles, 2006), may be expected to form part of the diet of the spiny hedgehogs in this area as well. Living forms such as *Erinaceus europaeus* and *Atelerix algirus* (e.g., on Balearic Islands; Reeve, 1994) are known to include small, thin-shelled snails into their diet. With its strong molar cusps and large basins, *A. steensmai* nov. sp. would have been able to also crack the shells of some of the larger and more strongly built snails relatively easily. In addition to small invertebrates, small reptiles such as lizards and snakes could have been part of the diet, with the processing of scales requiring distinct crunching activity. An ecological parallel can be made with relatively large-sized soricids such as *Amblycoptus* or *Beremendia*. For the former, a malacophagous and/or carnivore component has been suggested as well (Prieto and Van Dam, 2012; Van Dam, 2004). It might even be hypothesized that *Amblycoptus* was a direct competitor for the erinaceines, as the expansion of the former at the MN12-13 transition as recorded in the Teruel Basin coincides with the dwindling of the latter. A counter-argument against such a competitive relationship is their size difference, with length and width in *Amblycoptus* measuring about half those of the late Miocene Erinaceines (thereby approaching more that of older, middle Miocene erinaceines). The consumption of both gastropods and coleopterans has also been suggested for the Plio-Pleistocene soricid genus *Beremendia* (Furió et al., 2010).

The functional interpretation of rare known cranial material supports dental interpretations. A strong sagittal crest on the skull as observed in *Postpalerinaceus vireti* (Crusafont and De Villalta, 1947) fits both a diet including harder objects as well as softer vertebrate tissue (to slice through), because of the need for strong temporalis muscles to attach. *Amphechinus edwardsi* (Viret, 1938) also possesses such a crest, but its skull is narrower than in *P. vireti*, suggesting a lower degree of durophagy and/or carnassial action (as in bats; Freeman, 1984). Although the presence of a sagittal crest and various modifications in the dentition in more advanced erinaceines such as *Postpalerinaceus*, *Erinaceus* and *Atelerix* seem to point to a widening of the dietary spectrum including small vertebrates and/or hard objects, their mandibles do not show the typical modifications that characterize jaws of Carnivora. For instance, the position of the condyle is not low-positioned (approximately the level of the tooth row) as in carnivorans, but relatively high-positioned, as in insectivorans. This suggests that the position and structure of the condyle in erinaceines (and other insectivores) still allows for extra lateral movement in addition to the vertical movement required for shearing and/or crushing. On

the other hand, the possession of a thicker, ventrally slightly rounded jaw in advanced forms such as *Postpalerinaceus vireti* and *Erinaceus europaeus* would be consistent with the inclusion of harder items in the diet (beetles, small bone, shell, lizard shale), whereas thin jaws (*Amphechinus*) would point to the consumption of softer invertebrate food such as small insects, grubs, worms, etc. that could be probed and picked more easily using a long snout (Viret, 1938; Butler, 1948; see also Freeman, 1984, for a discussion on bats, and Van Dam et al., 2011, for a discussion on shrews).

Although biting force is expected to correspond to a larger coronoid process for the temporal muscles to attach (Turnbull, 1970), the inclination of the coronoid process with regard to the tooth row is perhaps not necessarily related to diet, as it might also depend on other, oppositely working evolutionary constraints such as tooth reduction. The inclination of the coronoid process also cannot be considered to be a very reliable taxonomic feature. For example, whereas the (anterior edge of the) coronoid process is inclined on the holotype of *P. vireti* (Crusafont and De Villalta, 1947: fig. 3), it is perpendicularly placed in the Cerro de Batallones material that supposedly belongs to the same species (Álvarez-Sierra et al., 2017: fig. 1). A similar ambiguity characterizes the mandible shape in *Amphechinus*, where the vertical ramus is almost vertical in *A. edwardsi* as described by Viret (1938: fig. 4), but positioned at an oblique angle (70–80°) in both *A. edwardsi* and *A. arvernensis* as described by Butler (1948: fig. 22). Based on an inclined ascending ramus in the mandible, Ziegler (2005b) preferred assignment of middle-sized erinaceine material from Hungary (Rudabanya, MN10) to *Postpalerinaceus* (*P. cingulatus*) rather than to the similarly-sized *Atelerix depereti*, the vertical ramus of which is perpendicularly placed (Depéret, 1887). Given the intra-generic variability of this character, the question of the generic assignment of '*P.*' *cingulatus* could be considered to be still open.

5.3. European Erinaceinae and Neogene climate change

According to terrestrial paleoclimate studies based on rodents, the entry of Erinaceinae (*Amphechinus*) in Spain at ~16 Ma would coincide with either a transition to drier conditions (Van der Meulen and Daams, 1992) or a generally dry period (Van Dam et al., 2006: suppl. fig. 7). New and updated precipitation estimates also point to relatively dry and open conditions between 18–14 Ma (Van Dam et al., ongoing work). The subsequent rarefaction of? *Amphechinus* during zone G (Van den Hoek Ostende and Furió, 2005; Furió et al., 2018) would be coeval with an increase in precipitation. In line with the hypothesis of a preference of erinaceines for more open and drier environments, renewed drying from 10 Ma corresponds to a rise of erinaceine occurrences (*Atelerix* aff. *depereti* and *Postpalerinaceus* cf. *vireti*) in the Teruel Basin – note that at the same time relatively wet-adapted groups such as soricids and gliroids disappear (Van Dam et al., 2001). A prolonged environmental deterioration seems finally also to have affected the Erinaceinae, however, which temporarily disappear from the area just before the time of the J2–J3 transition: despite the presence of well-documented upper J2 and J3 faunas such as Peralejos C, La Roma 1–2, and Masía de La Roma 604 (Van de Weerd, 1976; Van Dam et al., 2001; Alcalá et al., 2005), not a single occurrence of Erinaceinae has been recorded so far for the interval ~9.5–9.0 Ma. In fact, small-mammal diversity as a whole reaches a low, a development which is thought to correspond to the establishment of a truly dry summer (Van Dam, 2006).

The presence of various erinaceines during the early late Miocene MN9–10 in northeastern Spain (Vallès-Penedès Basin) seems to be at odds with the pattern described above, as conditions in this region were relatively wet at this time (Van Dam, 2006; Casanovas-Vilar and Agustí, 2007). Although the 'Vallesian crisis'

seems to have affected the erinaceines there as well (no record known after 9.4 Ma), their initial presence in this region requires an explanation. Perhaps '*A.*' *golpae*, a species only known from this area, differed from other erinaceines in preferring wetter or more closed environments. On the other hand, the occurrence of *Postpalerinaceus vireti* in both wetter sites such as Can Llobateres (Crusafont and Gibert, 1974), as well as in drier sites in the Teruel region points to a broad climatic tolerance, which could be linked to its diet, which supposedly includes a carnivorous component. The presence of yet another erinaceine species ('*P.*' *cingulatus*; Ziegler, 2005b) in the wetter central European site Rudabanya (Bernor et al., 2004; Van Dam and Utescher, 2016) further supports the notion of ecological differentiation within Miocene European spiny hedgehogs.

After a short absence between 9.5 and 8.8 Ma in the Teruel Basin, Erinaceinae presence resumes in Zone J4 (basal Turolian). Maximum erinaceine diversity is attained in Zone K (MN11, ca. 9–7.5 Ma), a period that is still relatively dry (Van Dam, 2006). The coexistence of various species during this interval could therefore be explained by a widening of dietary spectra (*Postpalerinaceus*, *A. steensmai*), including harder and larger invertebrates such as terrestrial gastropods, or small vertebrates with hard parts such as lizard scales. Alternatively, the occurrence of the latter species could be related to a temporary increase of humidity (early part of MN12; Van Dam and Weltje, 1999; van Dam, 2006).

The pattern of erinaceine diversification in the rest of Europe resembles that on the Iberian Peninsula, except for a number of significantly older occurrences (predominantly *Amphechinus*) as evidenced by the late Oligocene–early Miocene records of France and Germany. During the middle Miocene Erinaceinae constituted a rare but consistent element of well-sampled sites in Central and Eastern Europe (Hír et al., 2016; Prieto et al., 2015; Ziegler, 2005). Similarly, late middle Miocene erinaceines are well documented for France thanks to sites such as Sansan and La Grive. The late middle Miocene (MN7–8), an interval during which spiny hedgehogs were relatively rare in Spain, seems to have been a successful period for the group in France, Central Europe and Anatolia, with presences of *Postpalerinaceus*, *Atelerix* and *Mioechinus* (Engesser, 1980, 2009; Mein and Ginsburg, 2002). By contrast, the late Miocene record in Central Europe seems to be poorer than on the Iberian Peninsula, although a lower number of sites in the former region may cause some bias. The upper Miocene record of France is characterized by frequent occurrences (Mein, 1999).

It cannot be established with certainty whether the latest Miocene and Pliocene low in erinaceine diversity in the Iberian Peninsula reflects a pan-European phenomenon or not. Occasional occurrences are noted for the Pliocene of Central-Eastern Europe (e.g., Sulimski, 1962; Rzebik-Kowalska, 2002), with first entry of the modern genus *Erinaceus* (*E. samsonowiczii*) supposedly having taken place around the Miocene–Pliocene transition (Doukas et al., 1995). However, it is only during the Pleistocene that this genus starts to become relatively common.

New compilations of sea surface temperatures for the Mediterranean and Northern Atlantic show an episode of very strong cooling around ~7–6 Ma (Herbert et al., 2016). The sudden drops in temperature must have strongly affected environments in Europe and the Mediterranean region, areas that had remained very warm until then. It is tempting to link the strong decrease in Erinaceinae in the Mediterranean and Europe from the Messinian onwards to effects of this 'Messinian glaciation', perhaps in combination with renewed drying (van Dam, 2006). Although speculative, tectonic factors could have contributed to the demise of spiny hedgehogs in this period as well, given the evidence for accelerated uplift and basin formation across the Mediterranean region, including Iberia (Jolivet et al., 2006). The resulting

topographic barriers could have contributed to preventing spiny hedgehogs from returning to formerly inhabited areas.

The fact that *Atelerix* species are currently restricted to Africa is consistent with an important role of temperature on its past distribution. More generally, the combination of a preference for high temperatures and a tolerance towards aridity would fit the (semi-) desertic landscapes in which the majority of modern Erinaceinae species (*Hemiechinus*, *Paraechinus*, *Atelerix*) are currently thriving. As also suggested by Corbet (1988), a parallel may be drawn between the biogeographic histories of *Atelerix* and the ground squirrel *Atlantoxerus*, a common sciurid in the Iberian Peninsula during the Neogene until the Pliocene (García-Alix et al., 2007). Like the mainland distribution area of the northernmost living species of *Atelerix* (*A. algirus*), whose African presence can probably be traced back to the Plio-Pleistocene boundary (Butler, 2010), the geographic range of the only living species of *Atlantoxerus* (*A. getulus*) is restricted to northernmost Africa.

Acknowledgements

We are very grateful to Marta Palmero for making the specimen drawings. We thank Marc Furió for providing us with material of *Erinaceus europaeus* and his comments on the manuscript. We thank Marc Furió and Isaac Casanovas for their help with scanning specimens at the Department of Geology of the Universidad Autónoma de Barcelona, and Laura Celià and Marta March for consulting the ICP collection. We thank Eduardo Espilez, Emmanuel Robert and Wilma Wessels for their help in studying material from the Teruel, Lyon and Utrecht collections, respectively. Jérôme Prieto and Florentin Cailleux are thanked for their constructive reviews. We also greatly acknowledge the past efforts of Etienne Moissenet and Rafael Adrover in discovering, excavating and studying many of the fossil sites in the Teruel Basin. Research (J.A.v.D.) was funded by Generalitat de Catalunya (CERCA Program), and facilitated by Department of Earth Sciences, Utrecht University. Research (L.A.) of Group E04_17R FOCONTUR was financed by Departamento de Innovación, Investigación y Universidad (Gobierno de Aragón) and FEDER Aragón 2014-2020 ("Construyendo Europa desde Aragón").

References

- Adrover, R., 1974. Un relleno kárstico plio-pleistocénico en el Cerro de los Espejos en Sarrión (Prov. de Teruel, España) (Nota preliminar). *Acta Geológica Hispánica* 9, 142–143.
- Adrover, R., 1986. Nuevas faunas de roedores en el Mio-Plioceno continental de la región de Teruel (España). In: *Interés bioestratigráfico y paleoecológico. Instituto de Estudios Turolenses de la Excm. Diputación Provincial de Teruel, Teruel*.
- Ai, H.S., He, K., Chen, Z.Z., Li, J.Q., Wan, T., Li, Q., Nie, W.H., Wang, J.H., Su, W.T., Jiang, X.L., 2018. Taxonomic revision of the genus *Mesechinus* (Mammalia: Erinaceidae) with description of a new species. *Zoological Research* 39, 335–347.
- Albesa, J., Robles, F., 2006. Síntesis de los estudios sobre moluscos continentales neógenos del sector septentrional de la Depresión de Teruel: período 1775–1998. *Estudios Geológicos* 62, 183–198.
- Alcalá, L., Sesé, C., Herráez, E., Adrover, R., 1991. Mamíferos del Turoliense inferior de Puente Minero (Teruel, España). *Boletín de la Real Sociedad Española de Historia Natural (Sección Geológica)* 86, 205–251.
- Alcalá, L., Van Dam, J.A., Luque, L., Montoya, P., Abella, J., 2005. Nuevos mamíferos vallesienses en Masía de La Roma (Cuenca de Teruel). *Geogaceta* 37, 199–202.
- Álvarez-Sierra, M.A., García-Paredes, I., Gómez, A.R., Hernández-Ballarín, V., Van den Hoek Ostende, L.W., López-Antoñanzas, R., López-Guerrero, P., Oliver, A., Peláez-Campomanes, P., 2017. Los micromamíferos del Cerro de los Batallones. In: Morales, J., et al. (Eds.), *La colina de los Tigres Dientes de Sable: Los yacimientos miocenos del Cerro de los Batallones. Torrejón de Velasco, Madrid*, pp. 519–529.
- Andrews, P., Cook, J., 1990. *Owls, caves and fossils*. In: *Natural History Museum Publications. Natural History Museum, London*.
- Bernor, R.L., Kordos, L., Rook, L., Agustí, J., Andrews, P., Armour-Chelu, M., Begun, D.R., Cameron, D.W., Damuth, J., Daxner-Höck, G., De Bonis, L., Fejfar, O., Fessaha, N., Fortelius, M., Franzen, J., Gasparik, M., Gentry, A., Heissig, K., Heryak, N., Kaiser, T., Koufous, G.D., Krolopp, E., Jánosy, D., Llenas, M., Meszáros, L., Müller, P., Renne, P., Ročák, Z., Sen, S., Scott, R., Szyndlar, Z., Topál, G., Ungar,
- P.S., Utescher, T., Van Dam, J.A., Werdelin, L., Ziegler, R., 2004. Recent advances on multidisciplinary research at Rudabánya, late Miocene (MN9), Hungary: a compendium. *Palaeontographia Italica* 89, 3–36.
- Butler, P.M., 1948. On the evolution of the skull and teeth in the Erinaceidae, with special reference to fossil material in the British museum. In: *Proceedings of the Zoological Society of London*. 118, pp. 446–500.
- Butler, P.M., 1956. Erinaceidae from the Miocene of East Africa. *Fossil Mammals of Africa* 11, 1–75.
- Butler, P.M., 2010. Ch. 29. Neogene Insectivora. In: Werdelin, L., Sanders, W.J. (Eds.), *Cenozoic Mammals of Africa*. California University Press, Berkeley, pp. 573–580.
- Casanovas-Vilar, I., Agustí, J., 2007. Ecogeographical stability and climate forcing in the late Miocene (Vallesian) rodent record of Spain. *Palaeogeography, Palaeoclimatology, Palaeoecology* 248, 169–189.
- Corbet, G.B., 1988. The family Erinaceidae: a synthesis of its taxonomy, phylogeny, ecology and zoogeography. *Mammal Review* 18, 117–172.
- Crochet, J.Y., Heintz, E., 1971. Insectivora (Mammalia) de la faune villafranchienne de La Puebla de Valverde (prov. Teruel, Espagne). *Bulletin du Museum National d'Histoire Naturelle* 42, 776–779.
- Crusafont, M., Gibert, J., 1974. Nuevos datos sobre el género *Postpalerinaceus* del Vallesiense. *Acta Geologica Hispanica* 9, 1–3.
- Crusafont, M., De Villalta, J.F., 1947. Sur un nouveau *Palerinaceus* du Pontien d'Espagne. *Eclogae Geologicae Helveticae* 40, 320–333.
- Crusafont, M., De Villalta, J.F., Truyols, Y., 1955. El Burdigaliense continental de la cuenca del Vallés-Penedès. *Memorias y Comunicaciones del Instituto Geológico, Barcelona* 1–273, 12.
- Daams, R., Álvarez Sierra, M.A., Van der Meulen, A.J., Peláez-Campomanes, P., 1996. Paleoeology and paleoclimatology of micromammal faunas from upper Oligocene-lower Miocene sediments in the Loranca Basin, Province of Cuenca, Spain. In: Friend, P.F., Dabrio, C.J. (Eds.), *Tertiary Basins of Spain: the stratigraphic record of crustal kinematics*. Cambridge University Press, pp. 295–299.
- De Jong, F., 1988. Insectivora from the upper Aragonian and the lower Vallesian of the Daroca-Villafeliche area in the Calatayud-Teruel Basin (Spain). In: Freudenthal, M. (Ed.), *Biostratigraphy and paleoecology of the Neogene micromammalian faunas from the Calatayud-Teruel Basin (Spain)*. *Scripta Geologica Special Issue*. pp. 253–286.
- Depéret, C., 1887. Recherches sur la succession des faunes de vertébrés miocènes de la Vallée du Rhône. *Archives du Muséum d'Histoire naturelle de Lyon* 4, 1–269.
- Doukas, C.S., Van den Hoek Ostende, L.W., Theocharopoulos, C.D., Reumer, J.W.F., 1995. Insectivora. In: Schmidt-Kittler, N. (Ed.), *The vertebrate locality Maramea (Macedonia, Greece) at the Turolian-Ruscian boundary (Neogene)*. *Friedrich Pfeil, Munich*, pp. 43–64.
- Engesser, B., 1980. Insectivora und Chiroptera (Mammalia) aus dem Neogen der Türkei. *Schweizerische Paläontologische Abhandlungen* 102, 45–149.
- Engesser, B., 2009. The insectivores (Mammalia) from Sansan (middle Miocene, south-western France). *Schweizerische Paläontologische Abhandlungen* 128, 1–91.
- Freeman, P.W., 1979. Specialized insectivory: beetle-eating and moth-eating molossid bats. *Journal of Mammalogy* 60, 467–479.
- Freeman, P.W., 1984. Functional cranial analysis of large animalivorous bats (Microchiroptera). *Biological Journal of the Linnean Society* 21, 387–408.
- Freeman, P.W., 1992. Canine teeth of bats (Microchiroptera): size, shape and role in crack propagation. *Biological Journal of the Linnean Society* 45, 97–115.
- Freeman, P.W., 1998. Form, function and evolution in skulls and teeth of bats. In: Kunz, T.H., Racey, P.A. (Eds.), *Bat Biology and Conservation*. Smithsonian Institution Press, Washington, DC, pp. 140–156.
- Frost, D.R., Wozencraft, W.C., Hoffmann, R.S., 1991. Phylogenetic relationships of hedgehogs and gymnures (Mammalia: Insectivora: Erinaceidae). *Smithsonian Contributions to Zoology* 518, 1–69.
- Furió, M., Gibert, L., Ferrández, C., Sevilla, P., 2015. The insectivores (Soricidae, Erinaceidae; Eulipotyphla; Mammalia) from Cueva Victoria (Early Pleistocene, Murcia, Spain). *Neues Jahrbuch für Geologie und Paläontologie* 275, 151–161.
- Furió, M., Van den Hoek Ostende, L.W., Agustí, J., Minwer-Barakat, R., 2018. Evolution of the insectivore assemblages (Eulipotyphla, Mammalia) in Spain and their relation with Neogene and Quaternary climatic changes. *Ecosistemas* 27, 38–51.
- Furió, M., Agustí, J., Mouskhelishvili, A., Sanisidro, O., Santos-Cubedo, A., 2010. The paleobiology of the extinct venomous shrew *Beremendia* (Soricidae, Insectivora, Mammalia) in relation to the geology and paleoenvironment of Dmanisi (early Pleistocene, Georgia). *Journal of Vertebrate Paleontology* 30, 928–942.
- García-Alix, A., Minwer-Barakat, R., Martín Suárez, E., Freudenthal, M., 2007. New data on mio-pliocene Sciuridae (Rodentia, Mammalia) from Southern Spain. *Comptes Rendus Palevol* 6, 269–279.
- Gibert, J., 1975. New insectivores from the miocene of Spain; I and II. In: *Proceedings of the Koninklijke Nederlandse Akademie Van Wetenschappen, Series B*. 78, pp. 108–133.
- Gould, G.C., 2001. The phylogenetic resolving power of discrete dental morphology among extant hedgehogs and the implications for their fossil record. *American Museum Novitates* 3340, 1–52.
- Herbert, T.D., Lawrence, K.T., Tzanova, A., Peterson, L.C., Caballero-Gill, R., Kelly, C.S., 2016. Late Miocene global cooling and the rise of modern ecosystems. *Nature Geoscience* 9, 843–849.
- Hilgen, F.J., Lourens, L.J., Van Dam, J.A., 2012. The Neogene period. In: Gradstein, F.M., Ogg, J.G., Ogg, G. (Eds.), *A Geological Time Scale 2012*. Elsevier, Amsterdam, pp. 923–978.

- Hír, J., Venczel, M., Codrea, V., Angelone, C., Van den Hoek Ostende, L.W., Kirscher, U., Prieto, J., 2016. Badenian and Sarmatian s.str. from the Carpathian area: overview and ongoing research on Hungarian and Romanian small vertebrate evolution. *Comptes Rendus Palevol* 15, 863–875.
- Jolivet, L., Augier, R., Robin, C., Suc, J.-P., Jean Marie Rouchy, J.M., 2006. Lithospheric-scale geodynamic context of the Messinian salinity crisis. *Sedimentary Geology* 188–189, 9–33.
- López-Guerrero, P., García-Paredes, I., Van den Hoek Ostende, L.W., Van Dam, J.A., Álvarez-Sierra, M.Á., Hernández-Ballarín, V., Van der Meulen, A.J., Oliver, A., Peláez-Campomanes, P., 2011. Cañada: a new micromammal succession from the lower Vallesian of the Daroca area (Calatayud-Montalbán basin, Spain). *Estudios Geológicos* 67, 443–453.
- Lucas, P.W., 2004. *Dental Functional Morphology. How Teeth Work*. Cambridge University, Cambridge.
- Mein, P., 1999. The small mammal vallesian and turolian succession of France. In: Agustí, J., Rook, L., Andrews, P. (Eds.), *Evolution of Neogene terrestrial ecosystems in Europe*. Cambridge University Press, pp. 140–164.
- Mein, P., Ginsburg, L., 2002. Sur l'âge relatif des différents dépôts karstiques miocènes de La Grive-Saint-Alban (Isère). *Cahiers scientifiques – Muséum d'Histoire naturelle, Lyon* 2, 7–47.
- Mein, P., Martín-Suárez, E., 1994. *Galerix iberica* sp. nov. (Erinaceidae, Insectivora, Mammalia) from the late Miocene and early Pliocene of the Iberian Peninsula. *Geobios* 26, 723–730.
- Mein, P., Moissenet, E., Adrover, R., 1990. Biostratigraphie du Neogene supérieur du bassin de Teruel. *Paleontologia i Evolució* 23, 121–139.
- Opdyke, N., Mein, P., Lindsay, E., Pérez-González, A., Moissenet, E., Norton, V.L., 1997. Continental deposits, magnetostratigraphy and vertebrate paleontology, late Neogene of Eastern Spain. *Palaeogeography, Palaeoclimatology, Palaeoecology* 133, 129–148.
- Peláez-Campomanes, P., Morales, J., Álvarez Sierra, M.Á., Azanza, B., Fraile, S., García Paredes, I., Hernández Fernández, M., Herráez, E., Nieto, M., Pérez, B., Quirarte, V., Salesa, M.J., Sánchez, I.M., Soria, D., 2003. Updated biochronology of the Miocene mammal faunas from the Madrid basin (Spain). *Deinsea* 10, 431–441.
- Pfretschner, H.-U., 1997. Anpassung an der Zahnmorphologie an die Ernährung bei rezenten und fossilen Säugetieren. In: Alt, K.W., Türp, J.C. (Eds.), *Die Evolution Der Zähne - Phylogenie, Ontogenie, Variation*. Quintessenz Verlags-GmbH, Berlin, pp. 423–447.
- Piñero, P., Agustí, J., Oms, O., Blain, H.-A., Laplana, C., Ros-Montoya, S., Martínez-Navarro, B., 2017. Rodents from Baza-1 (Guadix-Baza Basin, Southeast Spain): filling the gap of the early Pliocene succession in the Betics. *Journal of Vertebrate Paleontology* 37, e1338294.
- Prieto, J., Van Dam, J.A., 2012. Primitive Anourosoricini and Allosoricinae from the Miocene of Germany. *Geobios* 45, 581–589.
- Prieto, J., Van den Hoek Ostende, L.W., Hír, J., Kordos, L., 2015. The middle miocene insectivores from Hasznos (Hungary, Nógrád County). *Palaeobiodiversity and Palaeoenvironments* 95, 431–451.
- Qiu, Z., 1996. *Middle Miocene Micromammalian Fauna From Tunggur, Nei Mongol*. Science Press Beijing, Beijing.
- Reeve, N., 1994. *Hedgehogs*. T. & A.D. Poyser, Ltd., London.
- Robles, F., Belinchón, M., García-Flor, J., Morales, J., 1991. El Neógeno continental de Buñol y del Valle del Río Cabriel. In: De Renzi, M., Márquez-Aliaga, A., Usera, J. (Eds.), *V Jornadas de Paleontología. El estudio de la forma orgánica y sus consecuencias en paleontología sistemática, paleoecología y paleontología evolutiva*. pp. 205–215.
- Rzebiak-Kowalska, B., 2002. The Pliocene and early Pleistocene Lipotyphla (Insectivora, Mammalia) from Romania. *Acta Zoologica Cracoviensis* 45, 251–281.
- Santana, E.M., Jantz, H.E., Best, T.L., 2010. *Atelerix albiventris* (Erinaceomorpha: Erinaceidae). *Mammalian Species* 42 (857), 99–110.
- Sulimski, A., 1962. Supplementary studies on the insectivores from Weże 1 (Poland). *Acta Paleontologica Polonica* 7, 441–498.
- Turnbull, W.D., 1970. *Mammalian Masticatory Apparatus*. 18, Fieldiana: Geology, pp. 147–356.
- Van Dam, J.A., 2004. Anourosoricini (Mammalia: Soricidae) from the Mediterranean region: a pre-Quaternary example of recurrent climate-controlled North-South range shifting. *Journal of Paleontology* 78, 741–764.
- Van Dam, J.A., 2006. Geographic and temporal patterns in the late Neogene (12–3 Ma) aridification of Europe: the use of small mammals paleoprecipitation proxies. *Palaeogeography, Palaeoclimatology, Palaeoecology* 238, 190–218.
- Van Dam, J.A., Utescher, T., 2016. Plant- and micromammal-based paleoprecipitation proxies: comparing results of the Coexistence and Climate-Diversity Approach. *Palaeogeography, Palaeoclimatology, Palaeoecology* 443, 18–33.
- Van Dam, J.A., Weltje, G.J., 1999. Reconstruction of the Late Miocene climate of Spain using rodent palaeocommunity successions; an application of end-member modelling. *Palaeogeography, Palaeoclimatology, Palaeoecology* 151, 267–305.
- Van Dam, J.A., Alcalá, L., Alonzo Zarza, A., Calvo, J.P., Garcés, M., Krijgsman, W., 2001. The Upper Miocene mammal record from the Teruel-Alfambra region (Spain). The MN system and continental Stage/Age concepts discussed. *Journal of Vertebrate Paleontology* 21, 367–385.
- Van Dam, J.A., Abdul Aziz, H., Álvarez Sierra, M.Á., Hilgen, F.J., Van den Hoek Ostende, L.W., Lourens, L.J., Mein, P., Van der Meulen, A.J., Peláez-Campomanes, P., 2006. Long-period astronomical forcing of mammal turnover. *Nature* 443, 687–691.
- Van Dam, J.A., Krijgsman, W., Abels, H.A., Álvarez-Sierra, M.Á., García-Paredes, I., López-Guerrero, P., Peláez-Campomanes, P., Ventura, D., 2014. Updated chronology for middle to late Miocene mammal sites of the Daroca area (Calatayud-Montalbán Basin, Spain). *Geobios* 47, 325–334.
- Van de Weerd, A., 1976. Rodent faunas of the Mio-Pliocene continental sediments of the Teruel-Alfambra region, Spain. *Utrecht Micropaleontological Bulletins Special Publication*, 2, pp. 1–217.
- Van den Hoek Ostende, L.W., 2003. Insectivores (Erinaceomorpha, Soricomorpha, Mammalia) from the Ramblan of the Daroca-Calamocha area. In: López-Martínez, N., Peláez-Campomanes, P., Hernández Fernández, M. (Eds.), *En torno a fósiles de mamíferos: datación, evolución y paleoambiente. Coloquios de Paleontología Volumen extraordinario*. 1, pp. 281–310.
- Van der Meulen, L.W., Furió, M., 2005. Spain. In: Vanden Hoek Ostende, L.W., Doukas, C.S., Reumer, J.W.F. (Eds.), *The Fossil Record of the Eurasian Neogene Insectivores (Erinaceomorpha, Soricomorpha, Mammalia)*, Part I. *Scripta Geologica, Special Issue* 5, pp. 148–284.
- Van der Meulen, A.J., García-Paredes, I., Álvarez-Sierra, M.A., Van den Hoek Ostende, L.W., Hordijk, K., Oliver, A., Peláez-Campomanes, P., 2012. Updated Aragonian biostratigraphy: small mammal distribution and its implications for the Miocene European chronology. *Geologica Acta* 10, 159–179.
- Van Der Meulen, A.J., Daams, R., 1992. Evolution of early-middle Miocene rodent faunas in relation to long-term palaeoenvironmental changes. *Palaeogeography, Palaeoclimatology, Palaeoecology* 93, 227–253.
- Van Valkenburgh, B., Ruff, C.B., 1987. Canine tooth strength and killing behavior in large carnivores. *Journal of Zoology, London* 212, 379–397.
- Viret, J., 1938. Étude sur quelques érinacéidés fossiles spécialement sur le genre *Palaerinaecus*. *Travaux du laboratoire de Géologie de la Faculté des Sciences de Lyon* 34, 1–32.
- Ziegler, R., 1999. Order insectivora. In: Roessner, G.E., Heissig, K., Fahlbusch, V. (Eds.), *The Miocene Land Mammals of Europe*. Federal Republic of Germany, Pfeil, Munich, pp. 53–74.
- Ziegler, R., 2005a. Erinaceidae and Dimylidae (Lipotyphla) from the late Middle Miocene of South Germany. *Senckenbergiana Lethaea* 85, 131–152.
- Ziegler, R., 2005b. The insectivores (Erinaceomorpha and Soricomorpha, Mammalia) from the Late Miocene hominoid locality Rudabánya. *Palaeontographia Italica* 90, 53–81.
- Ziegler, R., Dahlmann, T., Storch, G., 2007. Marsupialia, Erinaceomorpha and Soricomorpha (Mammalia). In: Daxner-Höck, G. (Ed.), *Oligocene-Miocene Vertebrates from the Valley of Lakes (Central Mongolia): Morphology, phylogenetic and stratigraphic implications*. *Annalen des Naturhistorischen Museums in Wien* 108A, pp. 53–164.